Supporting Information

Table of Contents

1H NMR spectra

6,6'-((1*E*,1'*E*)-(ethane-1,2-diylbis(azaneylylidene))bis(methaneylylidene))bis(3,5-di-tert-butylbenzene-1,2-diol) (**1**)

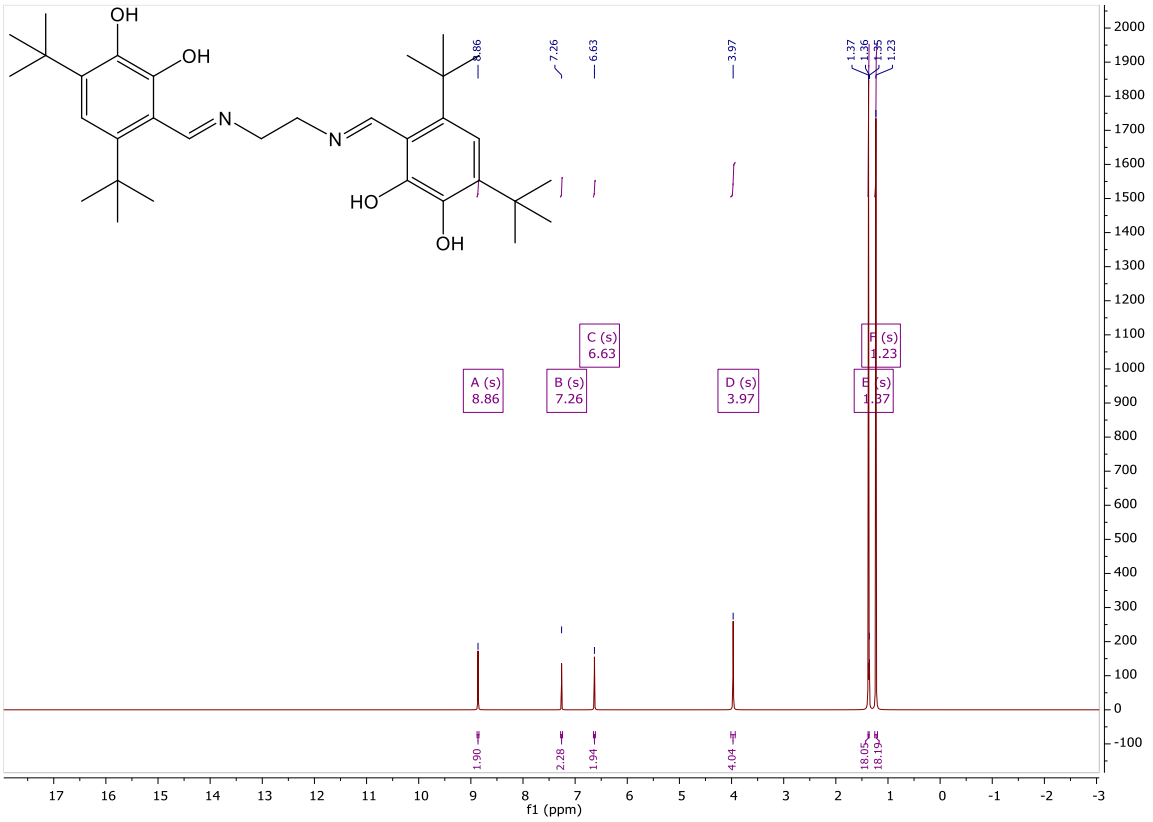

6,6'-((1*E*,1'*E*)-(propane-1,3-diylbis(azaneylylidene))bis(methaneylylidene))bis(3,5-di-tert-butylbenzene-1,2-diol) (**2**)

4,6-di-tert-butyl-3-((pyridin-4-ylimino)methyl)benzene-1,2-diol (**3**)

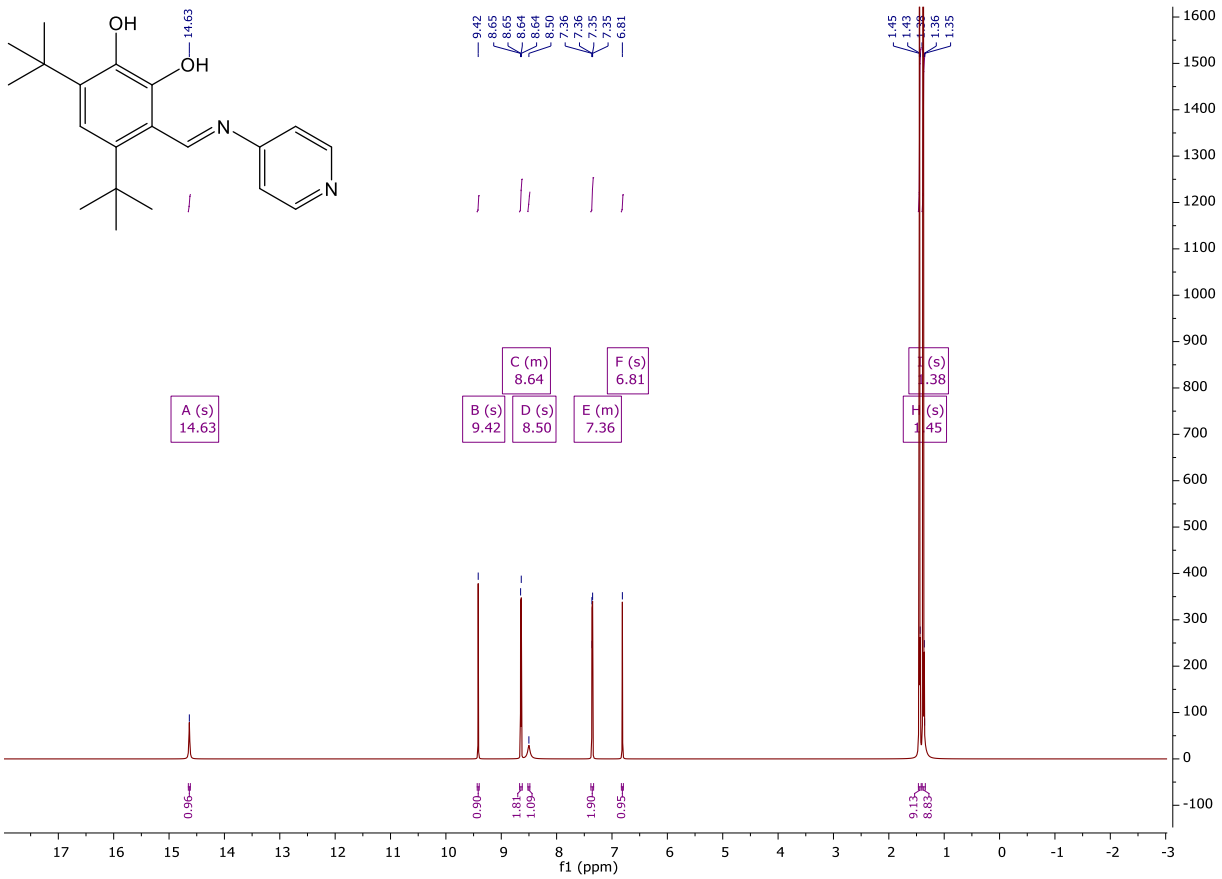

4-((4,6-di-tert-butyl-2,3-dihydroxybenzylidene)amino)benzenesulfonamide (**5**)

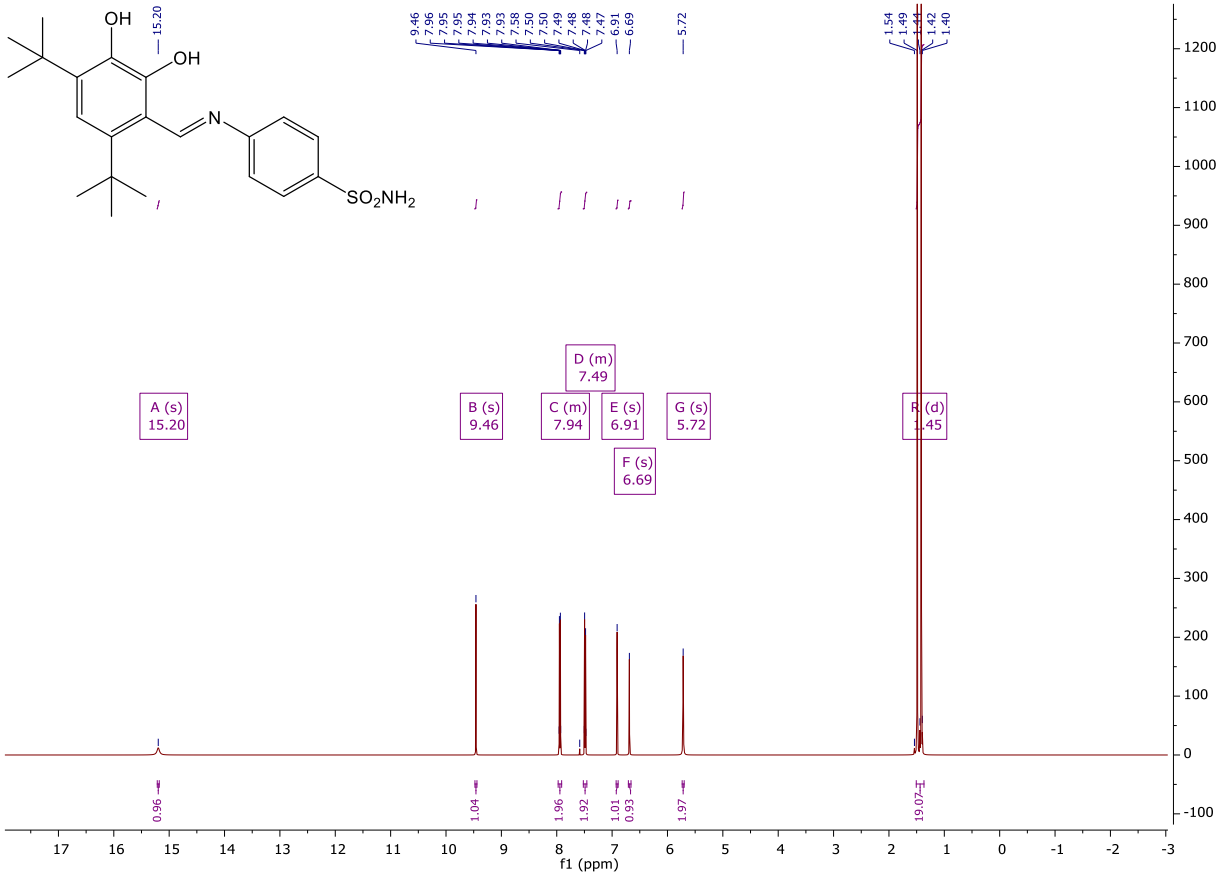

4,6-di-tert-butyl-3-(((4-hydroxyphenyl)imino)methyl)benzene-1,2-diol (**6**)

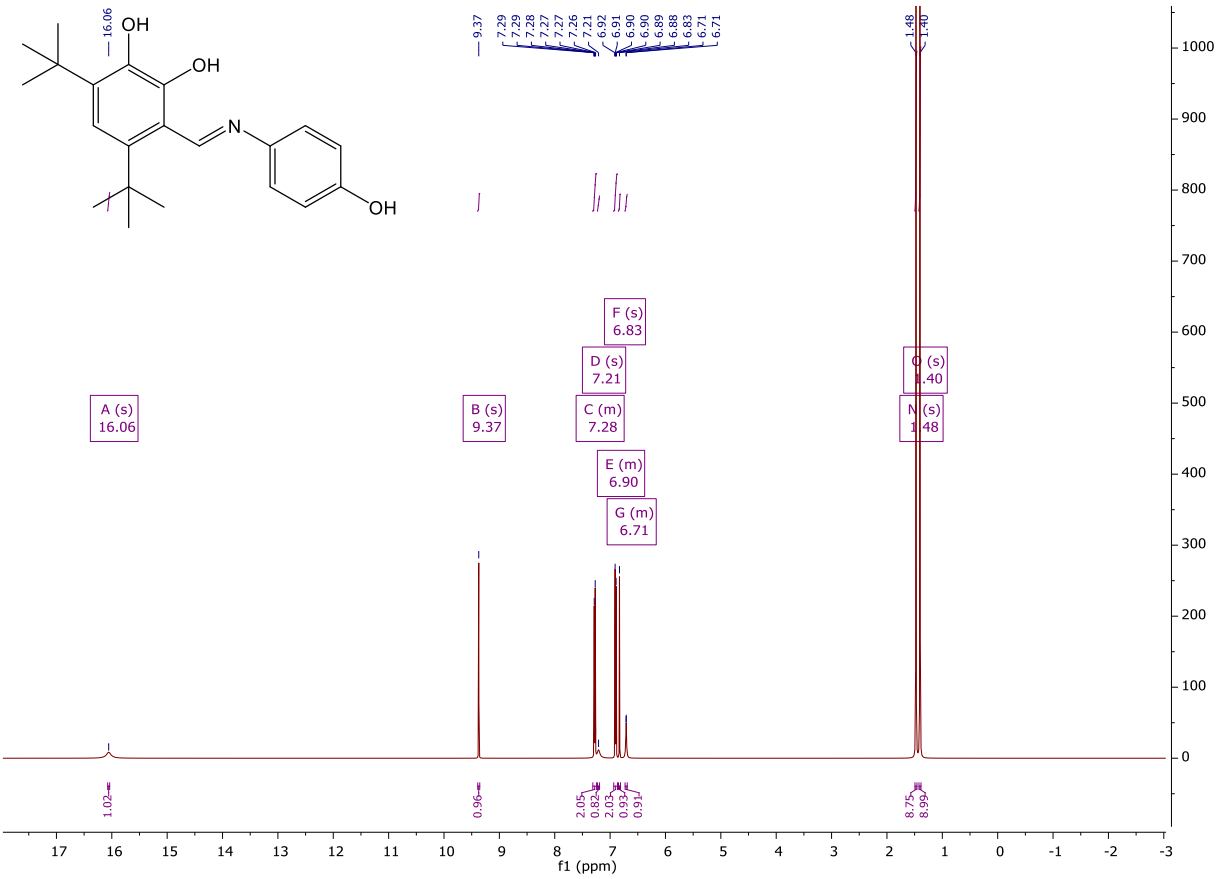

FT-IR spectra

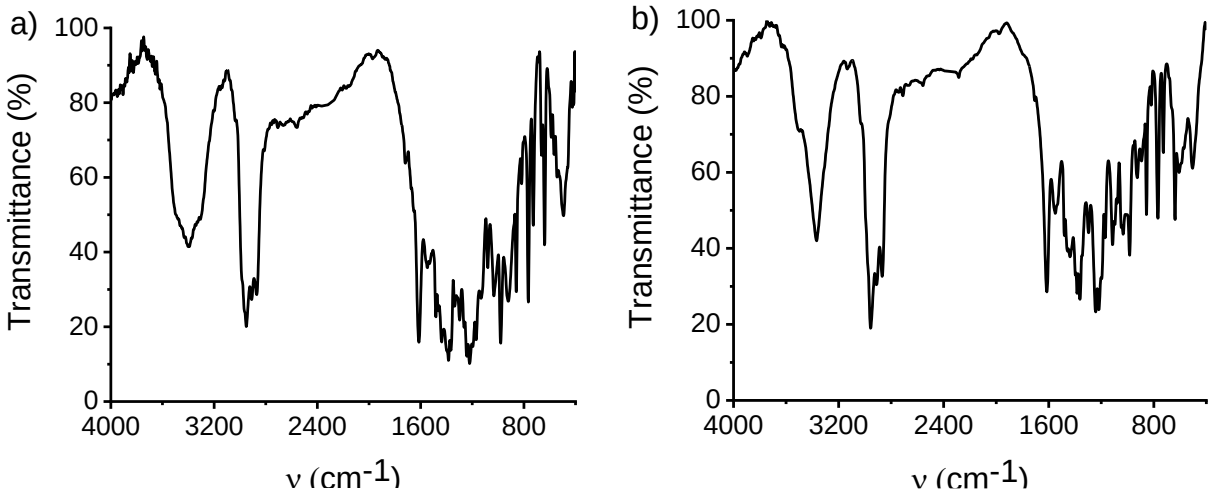

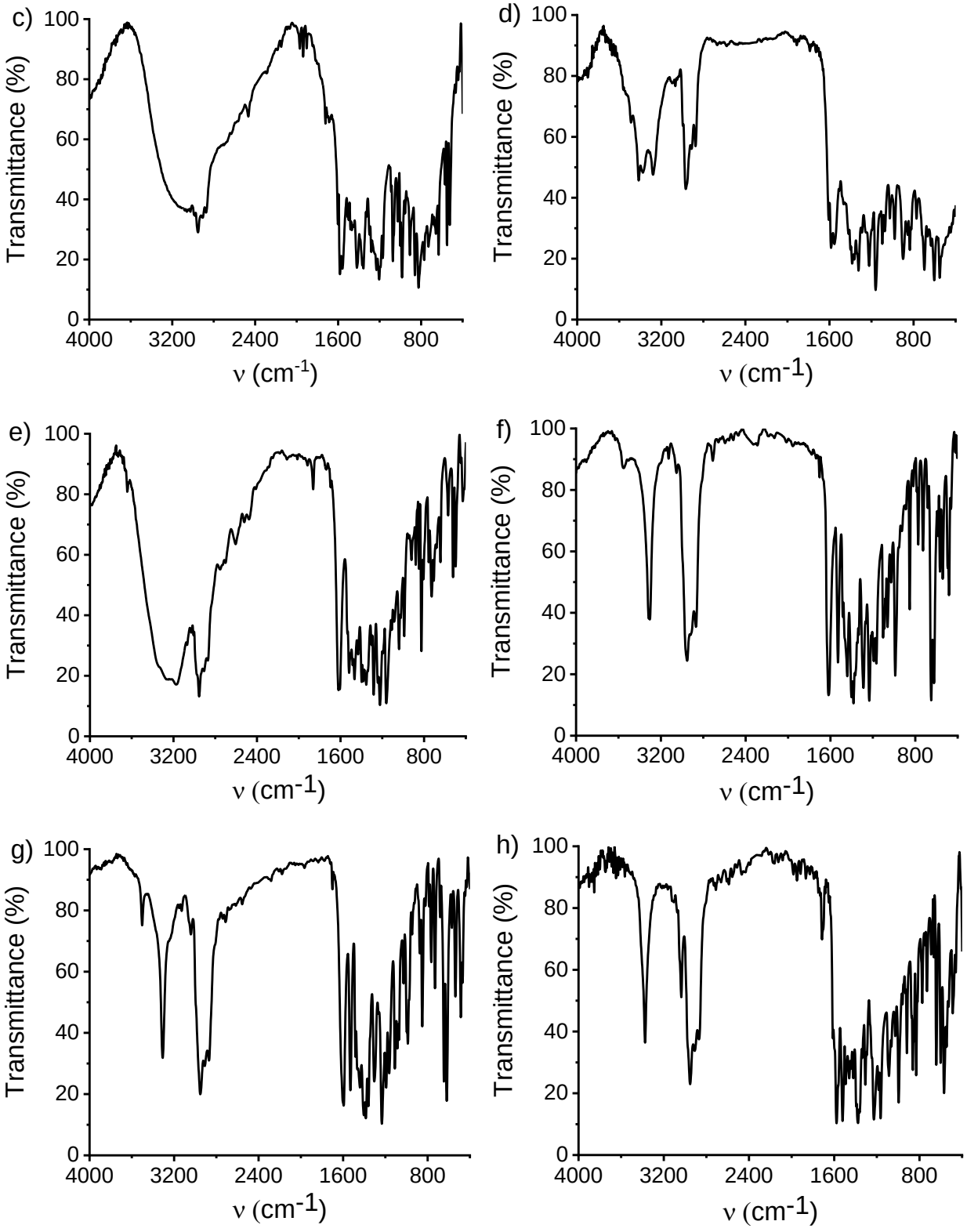
c)
d)
e)
f)
g)
h)
Transmittance (%)
100
80
60
40
20
0
4000
3200
2400
1600
800
ν (cm-1)

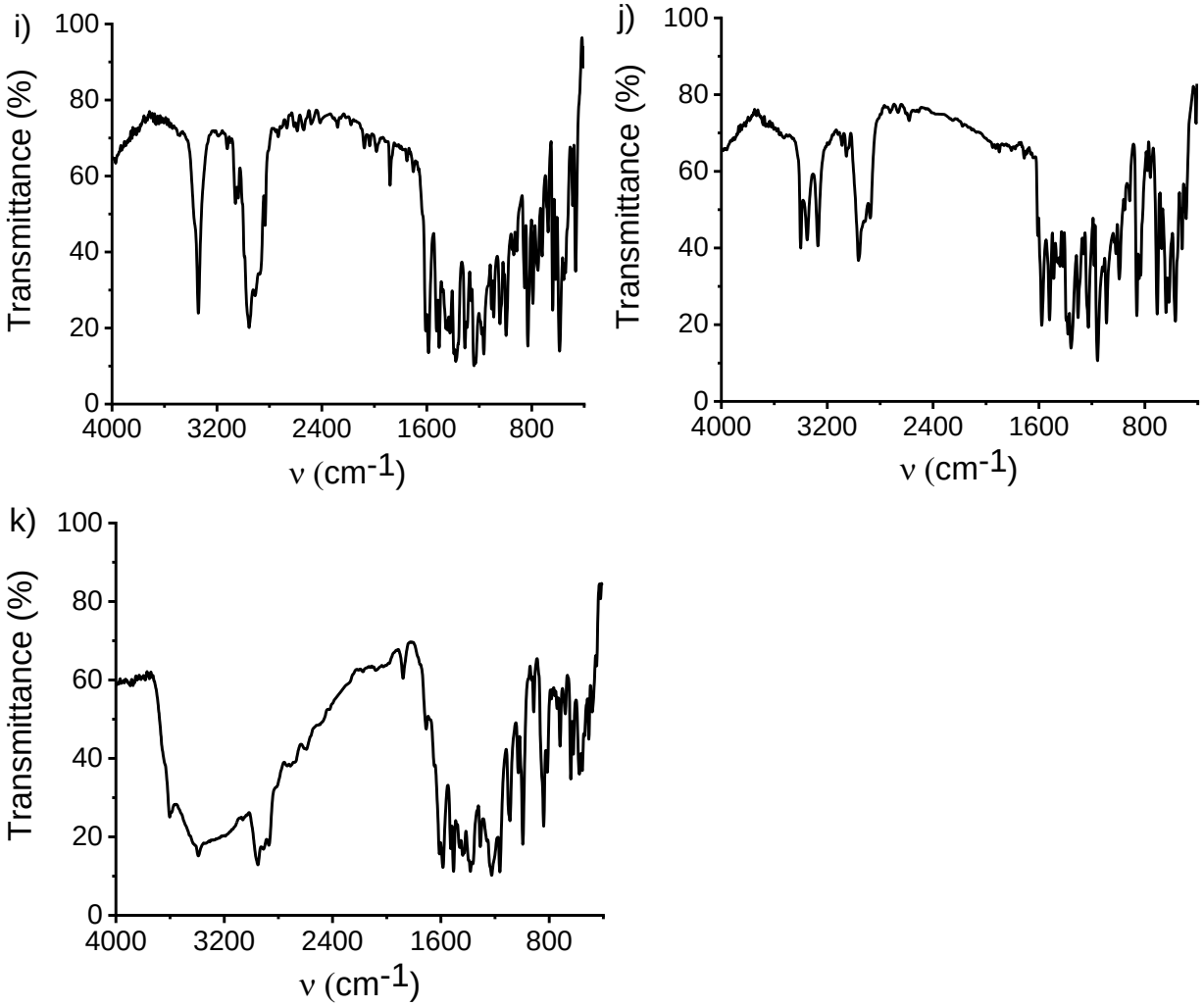

Figure S1. FT-IR spectra of the ligands **1** (a), **2** (b), **3** (c), **5** (d), **6** (e) and their Cu(II) complexes **1a** (f), **2a** (g), **3a** (h), **4a** (i), **5a** (j), **6a** (k). FT-IR spectrum of the ligand **4** is given in [1].

UV-vis spectra

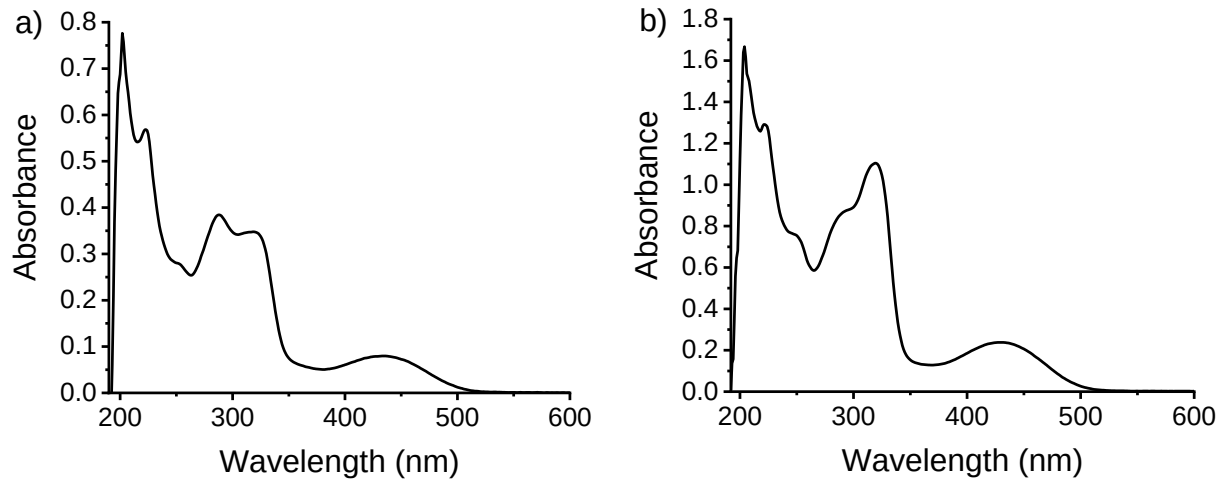

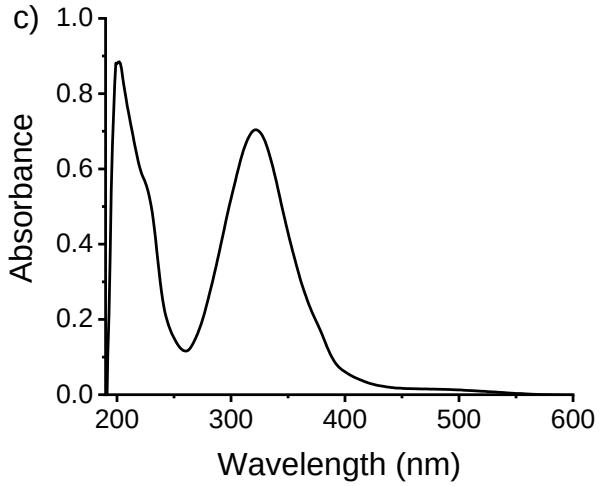
c)
Absorbance
Wavelength (nm)

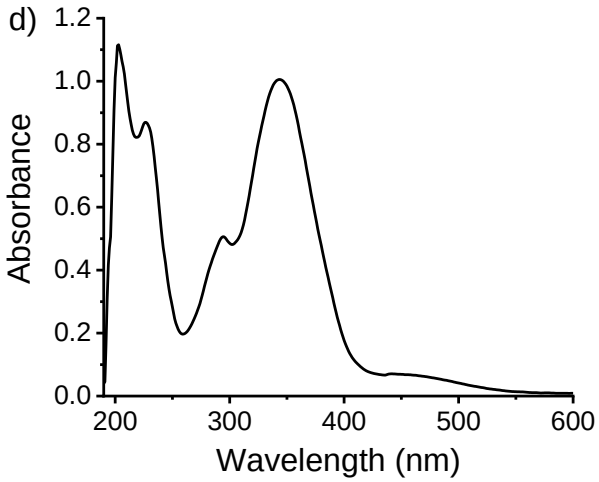
d)
Absorbance
Wavelength (nm)

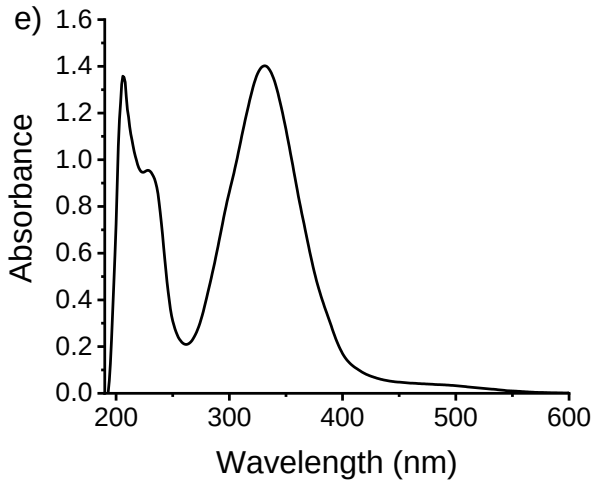
e)
Absorbance
Wavelength (nm)

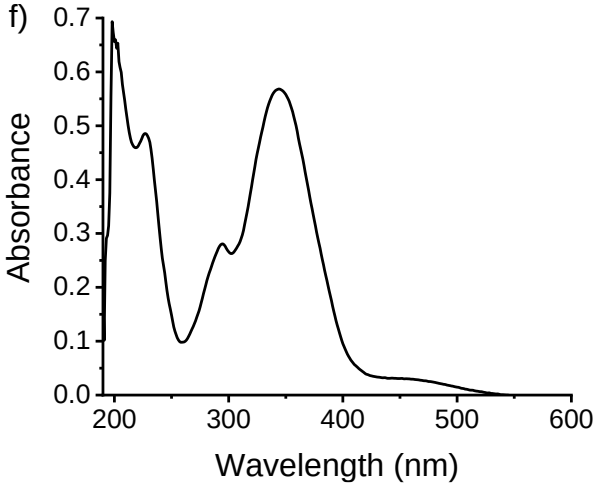
f)
Absorbance
Wavelength (nm)

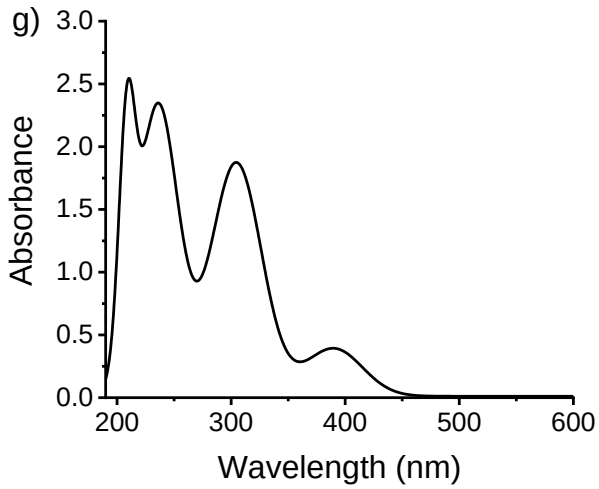
g)
Absorbance
Wavelength (nm)

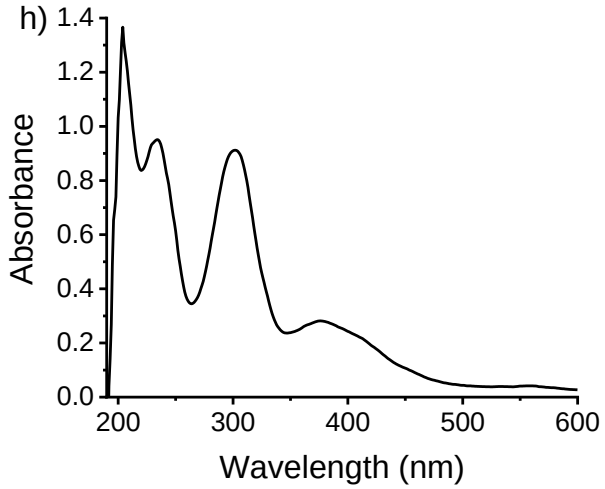
h)
Absorbance
Wavelength (nm)

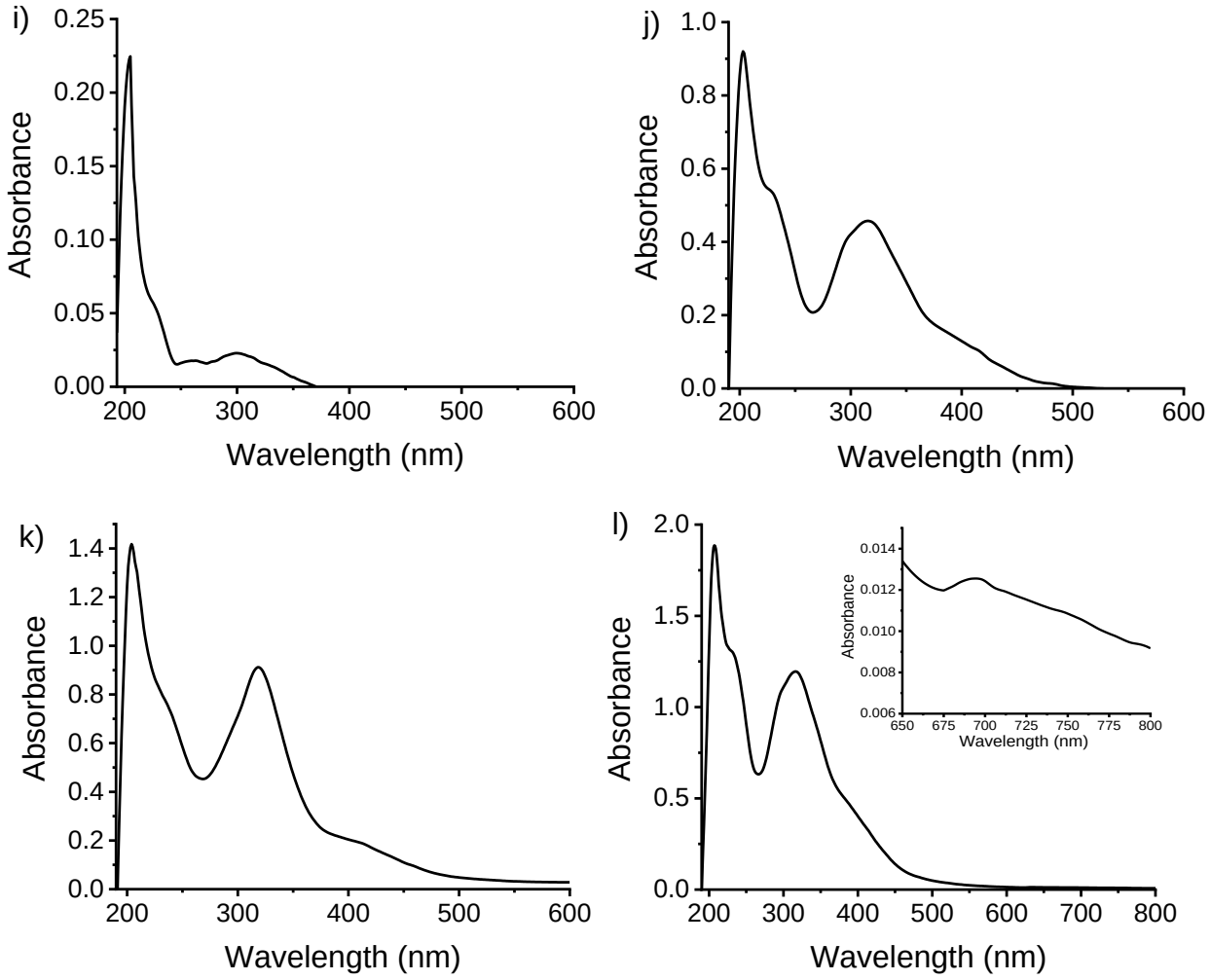

Figure S2. UV-Vis spectra of the ligands **1** (a; 85 μM), **2** (b; 59 μM), **3** (c; 74 μM), **4** (d; 48 μM), **5** (e; 91 μM), **6** (f; 34 μM) and their Cu(II) complexes **1a** (g; 81 μM), **2a** (h; 64 μM), **3a** (i; 122 μM), **4a** (j; 41 μM), **5a** (k; 23 μM), **6a** (l; 53 μM) in acetonitrile solutions.

X-Ray diffractograms

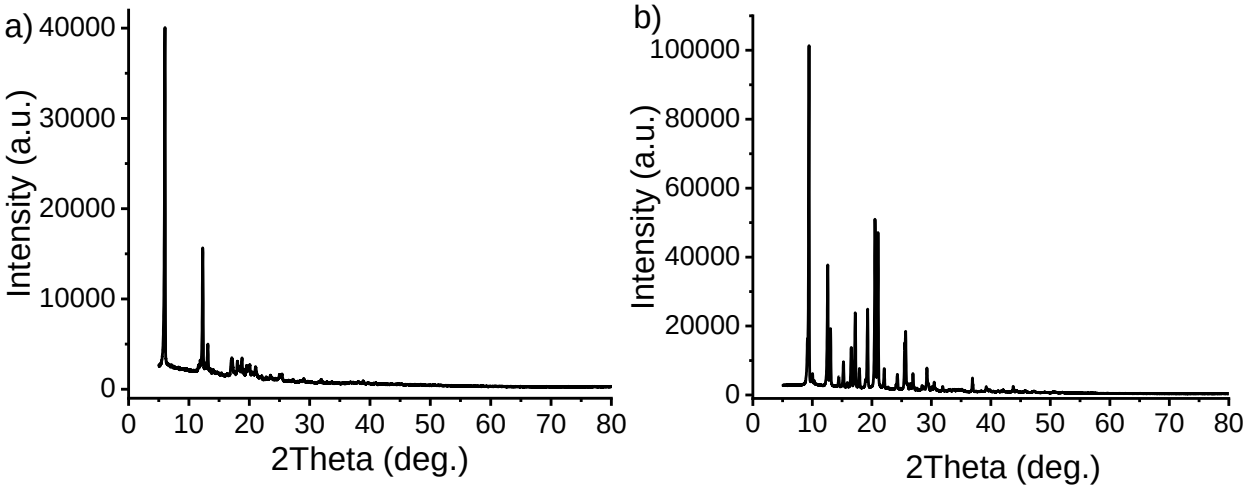

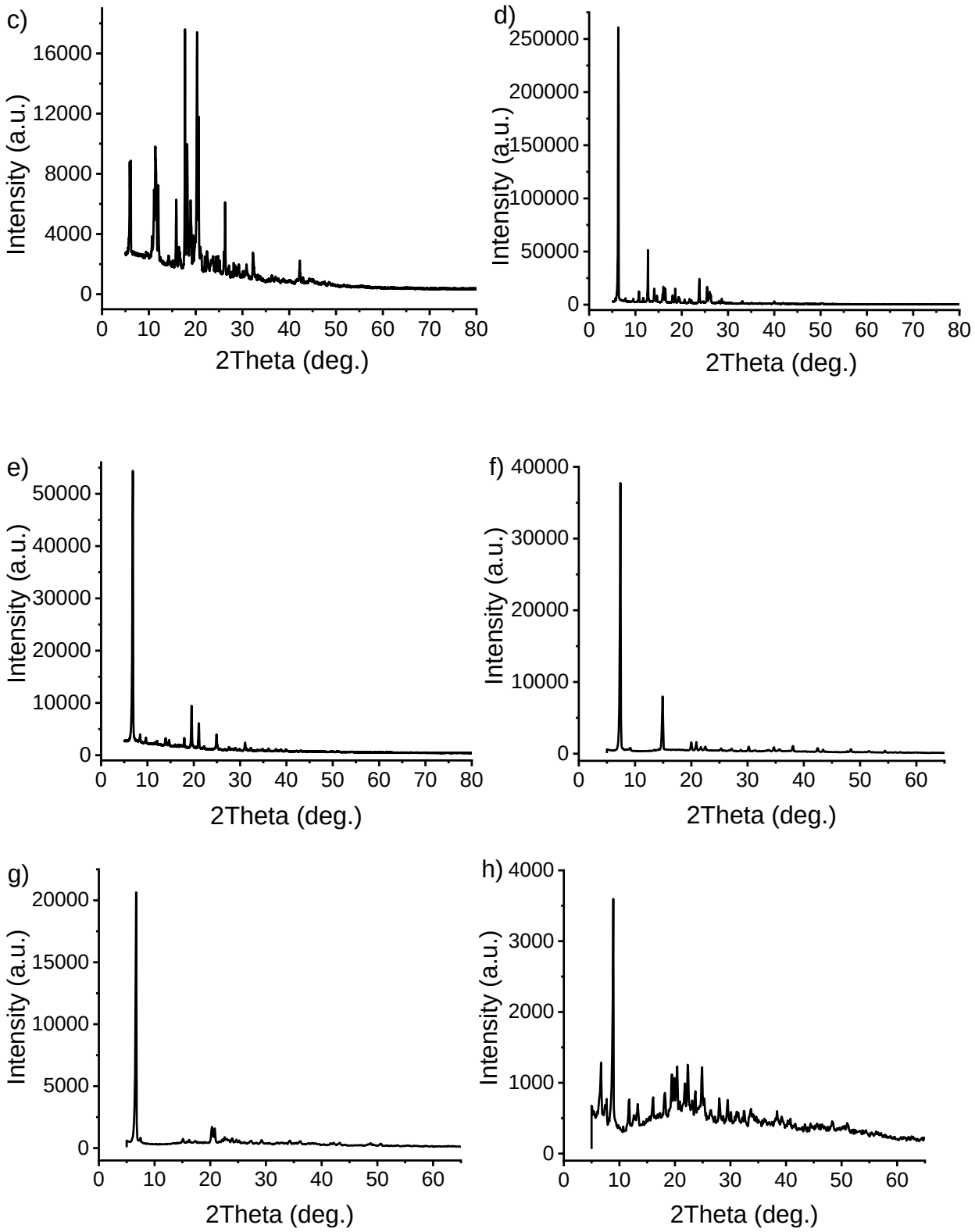

Figure S3. X-Ray diffractograms of the ligands **2** (a), **4** (b), **5** (c), **6** (d) and their Cu(II) complexes **2a** (e), **4a** (f), **5a** (g), **6a** (h).

ESR spectra

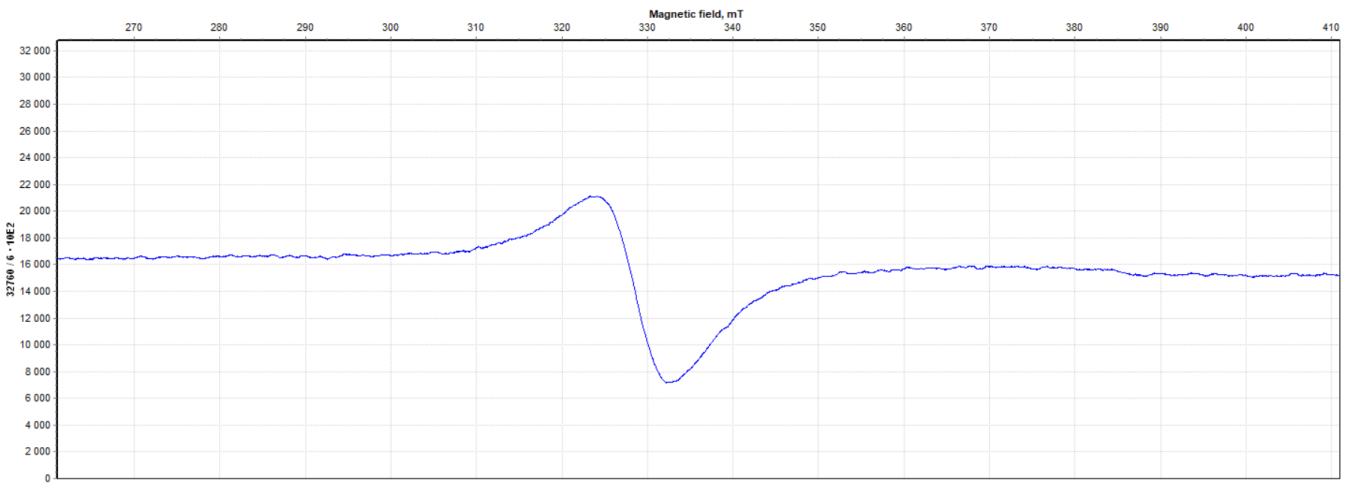

Figure S4. ESR spectrum of the Cu(II) complex **3a**.

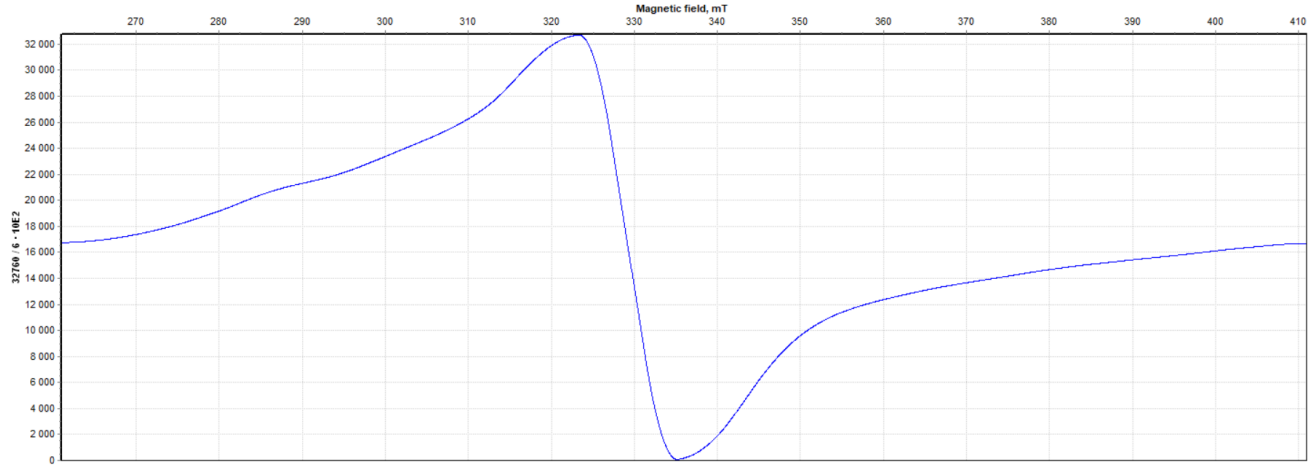

Figure S5. ESR spectrum of the Cu(II) complex **4a**.

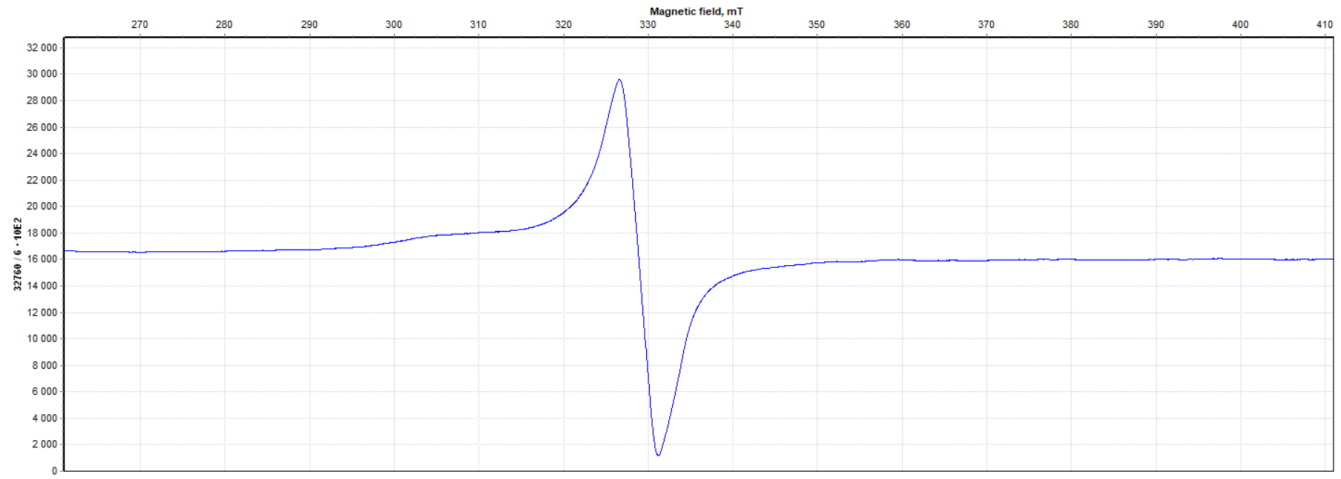

Figure S6. ESR spectrum of the Cu(II) complex **5a**.

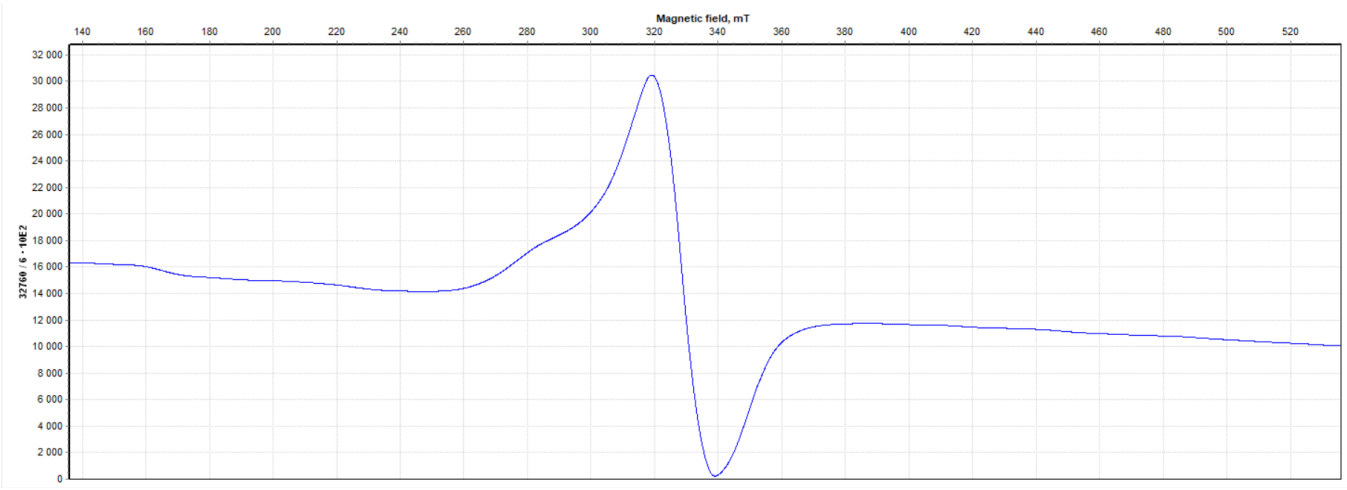

Figure S7. ESR spectrum of the Cu(II) complex **6a**.

TG and DSC curves

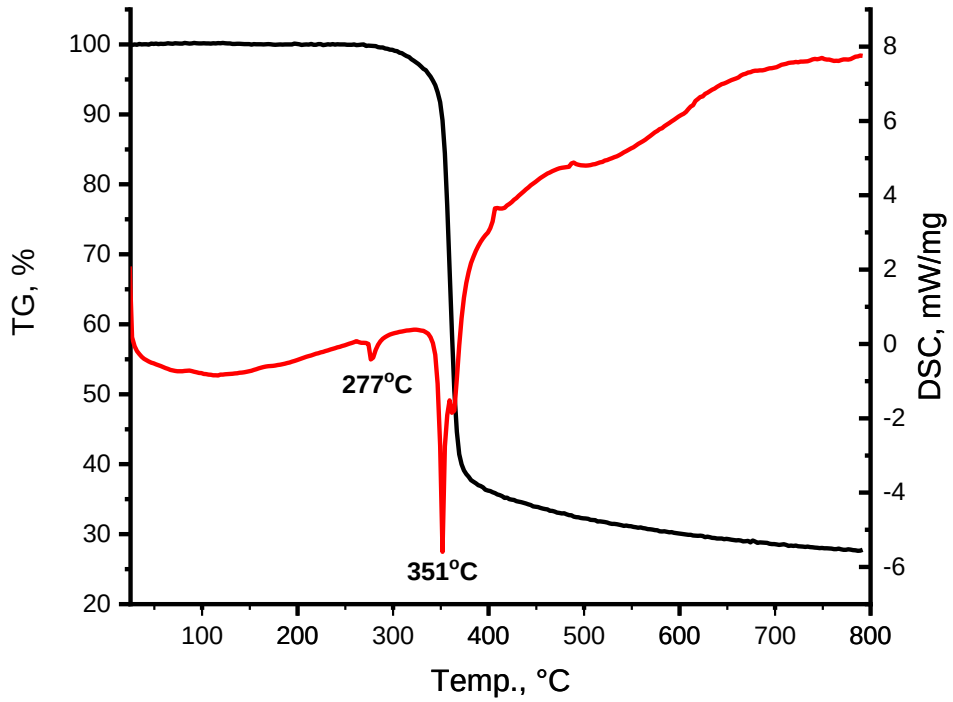

Figure S8. TG and DSC curves of the compound **1a**.

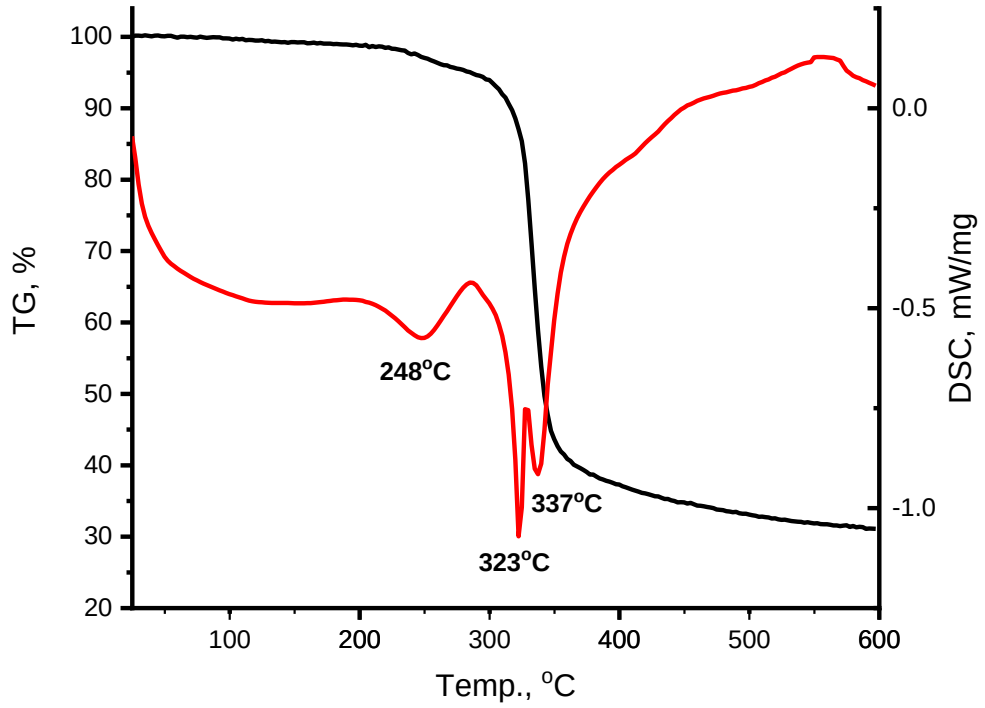

Figure S9. TG and DSC curves of the compound **2a**.

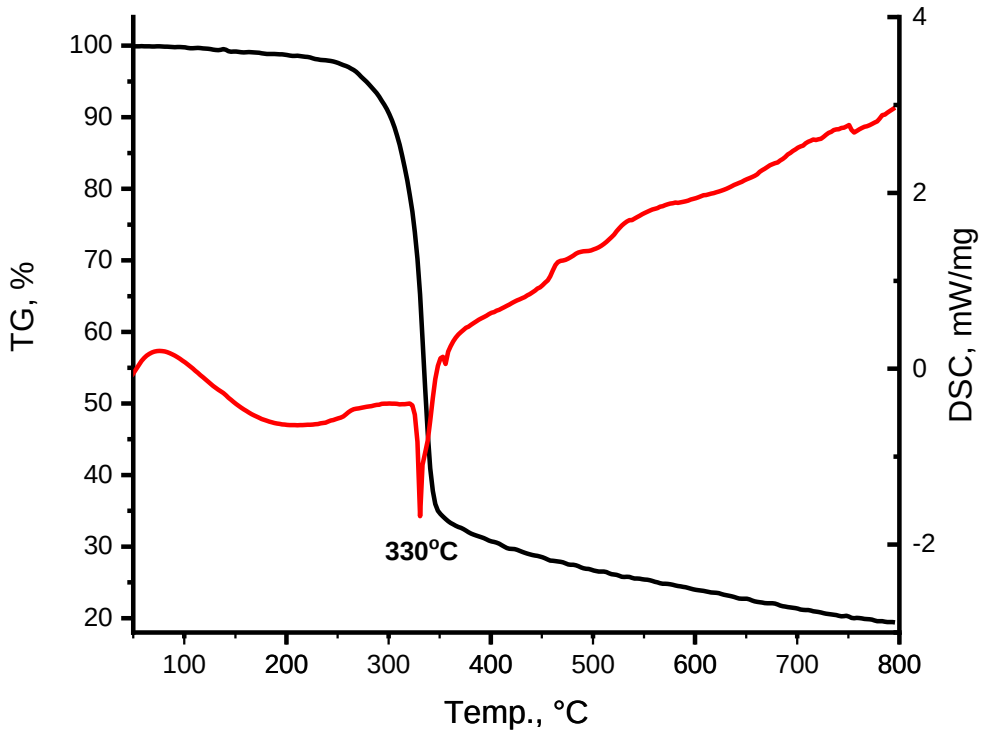

Figure S10. TG and DSC curves of the compound **3a**.

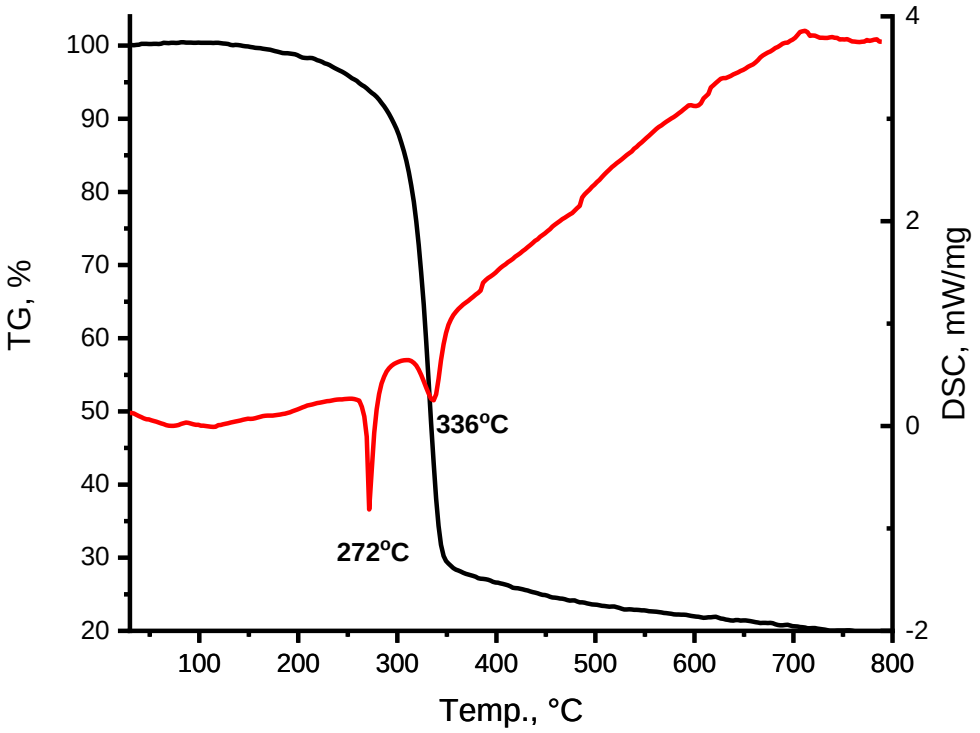

Figure S11. TG and DSC curves of the compound **4a**.

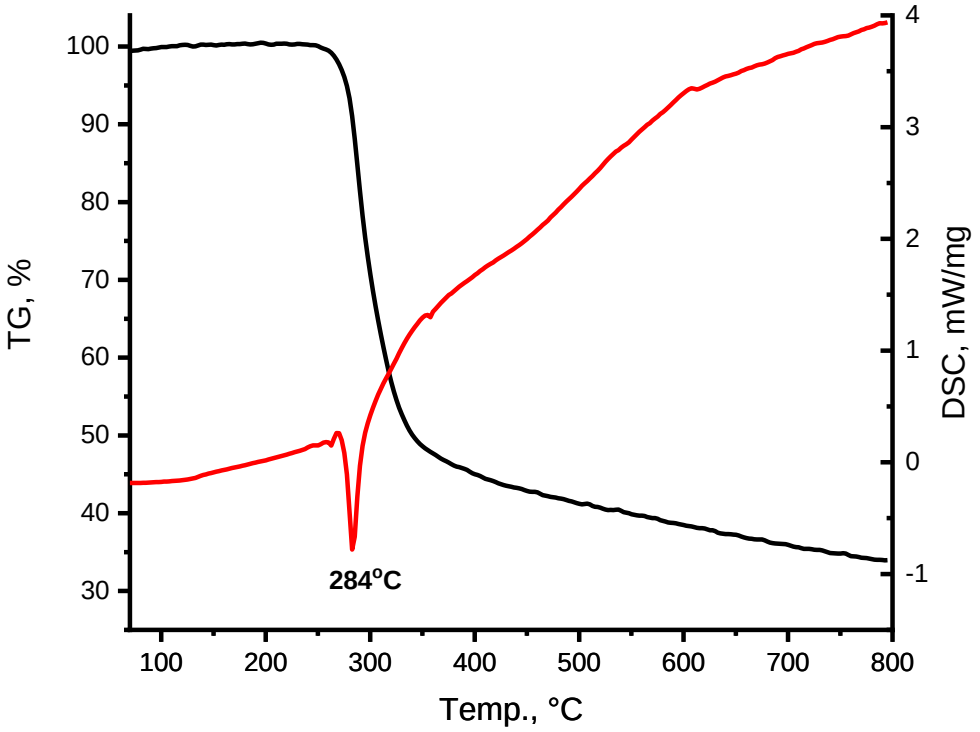

Figure S12. TG and DSC curves of the compound **5a**.

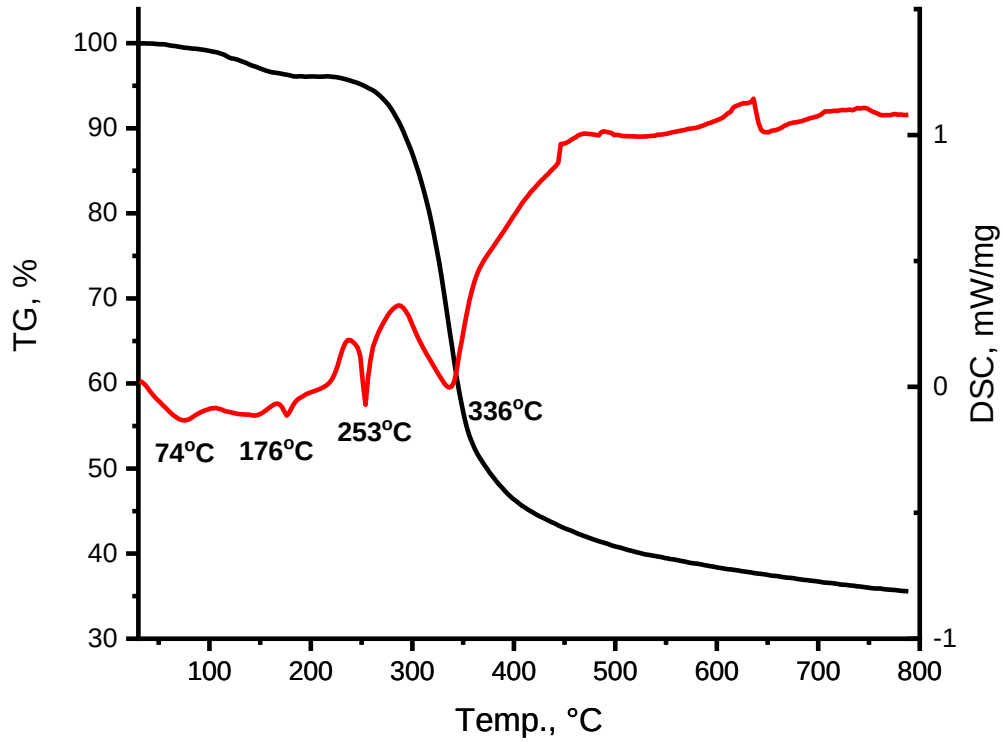

Figure S13. TG and DSC curves of the compound **6a**.

Table S1. Thermal properties of the compounds.

sample	Td[a], °C	Mass after destruction, %	Energy of thermal destruction, J/g
1a	335	28	-150.9
2a	285	31	-137.0
3a	280	19	-104.6
4a	258	21	-90.0
5a	277	36	-119.0
6a	299[b]	34	-140.3

[a] Temperatures of destruction (Td) were calculated as 5% weight loss.

[b] Due to the presence of solvent in the complex, the destruction temperature (Td) was calculated according to the instrument software.

ESI-MS spectra

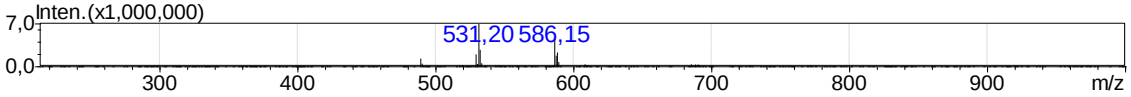

Figure S14. ESI-MS(+) spectrum of the Cu(II) complex **1a**.

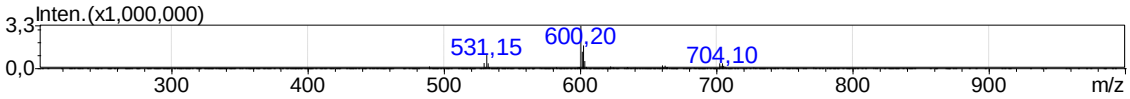

Figure S15. ESI-MS(+) spectrum of the Cu(II) complex **2a**.

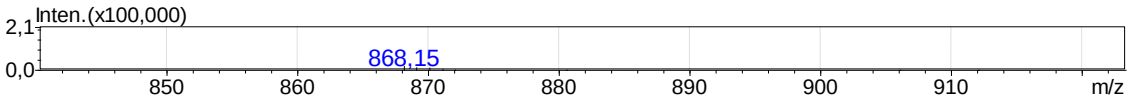

Figure S16. ESI-MS(–) spectrum of the Cu(II) complex **5a**.

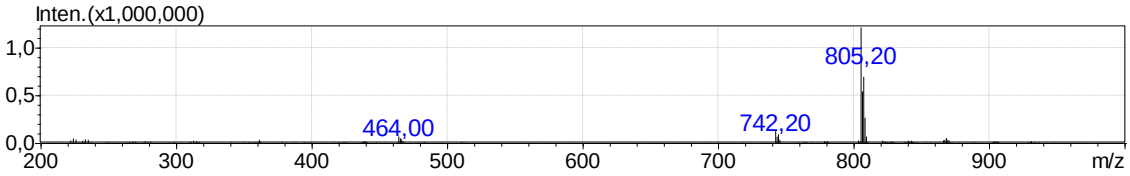

Figure S17. ESI-MS(–) spectrum of the Cu(II) complex **6a**.

Electrochemistry

Table S2. Cyclic voltammetry data (anodic, cathodic scan, 50 mV · s^{-1}) for the ligands and their Cu(II) complexes.

Compound	Anodic scan, E_{pa}, V					Cathodic scan, E_{pc}, V		
1	0.91	1.12	1.40	1.63	2.06	-1.78	~-2.5	
1a	0.91	1.29	1.41	1.67	2.08	-0.63	-1.11	
2	0.88	1.63	2.03			-1.80		
2a	0.96	1.59				-0.72	-1.1	
3	0.71	1.17	1.83					
4	0.82	1.11	1.48	1.63	1.94	-1.56		
4a	0.83	1.37	1.60	1.89		-0.75		
5	0.94	1.10	1.39	1.61	2.02	-1.31	-1.92	-2.23
5a	0.91	1.03	1.39	1.57	2.01	-1.42		
6	0.81	1.08	1.36	1.67	1.89	-1.61	-1.83	
6a	0.85		1.35	1.66	1.91	-0.65	-1.04	-1.83

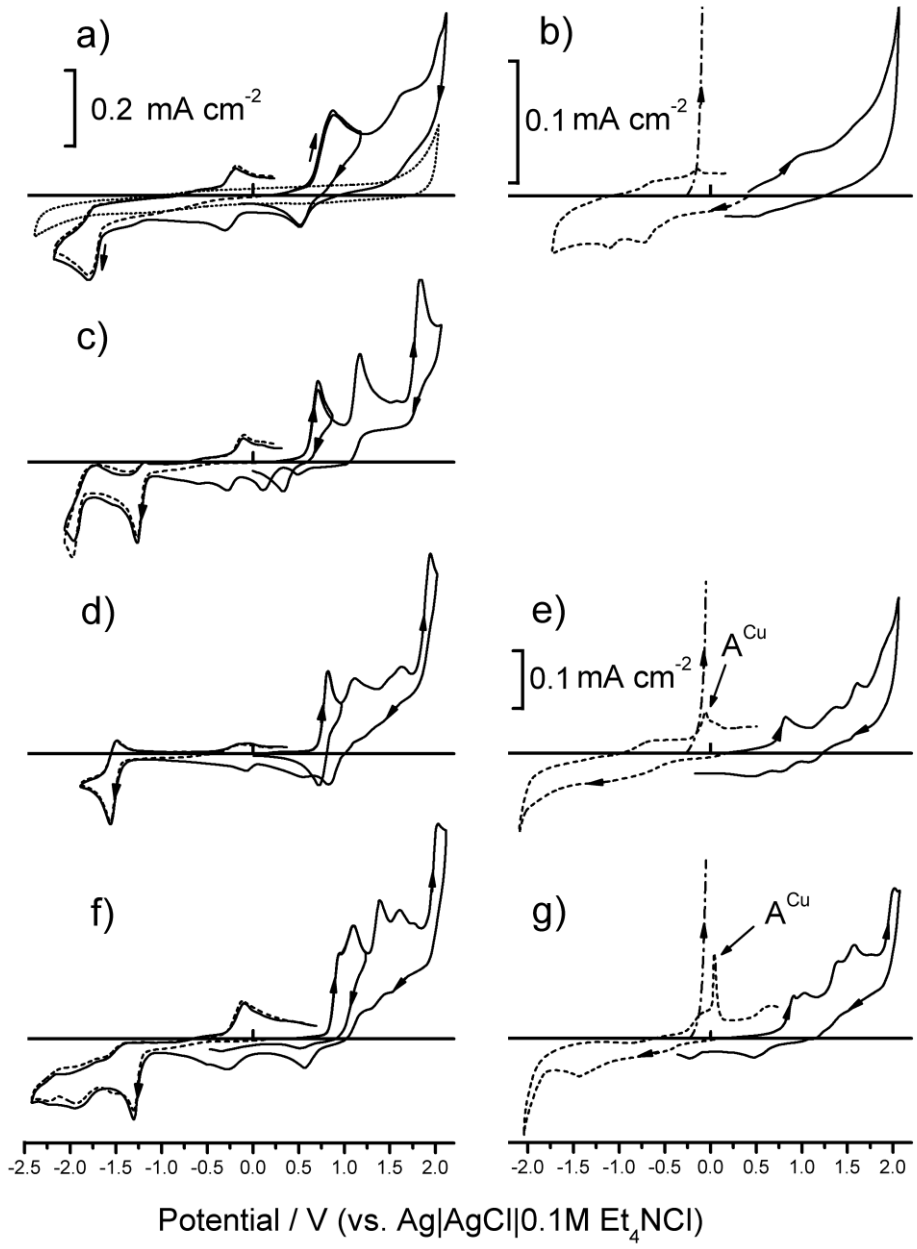

Figure S18. Voltammograms (50 mV/s) of the ligands **2** (a), **3** (c), **4** (d), **5** (f) (1.36 mmol·l^{-1}) and their complexes **2a** (b), **4a** (e), **5a** (g) (0.7 mmol·l^{-1}) upon anodic polarization (*solid line*), cathodic polarization (*dashed line*) in 0.1 mol·l^{-1} $(C_2H_5)_4NClO_4$ acetonitrile solution on glassy-carbon electrode and background cyclic voltammogram of glassy-carbon electrode (*dotted line*), anodic voltammogram of copper electrode (*dashed-dotted line*). *For the complexes **2a** and **4a** the concentrations are approximately 0.15мM and 0.3-0.4 мM, respectively, due to their low solubility.

Protein binding studies

The formula used for the plotting and analysis of protein binding data [2]:

$$\frac{F_0 - F}{F_0 - F_s} = \frac{[P] + [Q] + K_d - \sqrt{([P] + [Q] + K_d)^2 - 4[P][Q]))}}{2[P]}$$

Albumin binding studies

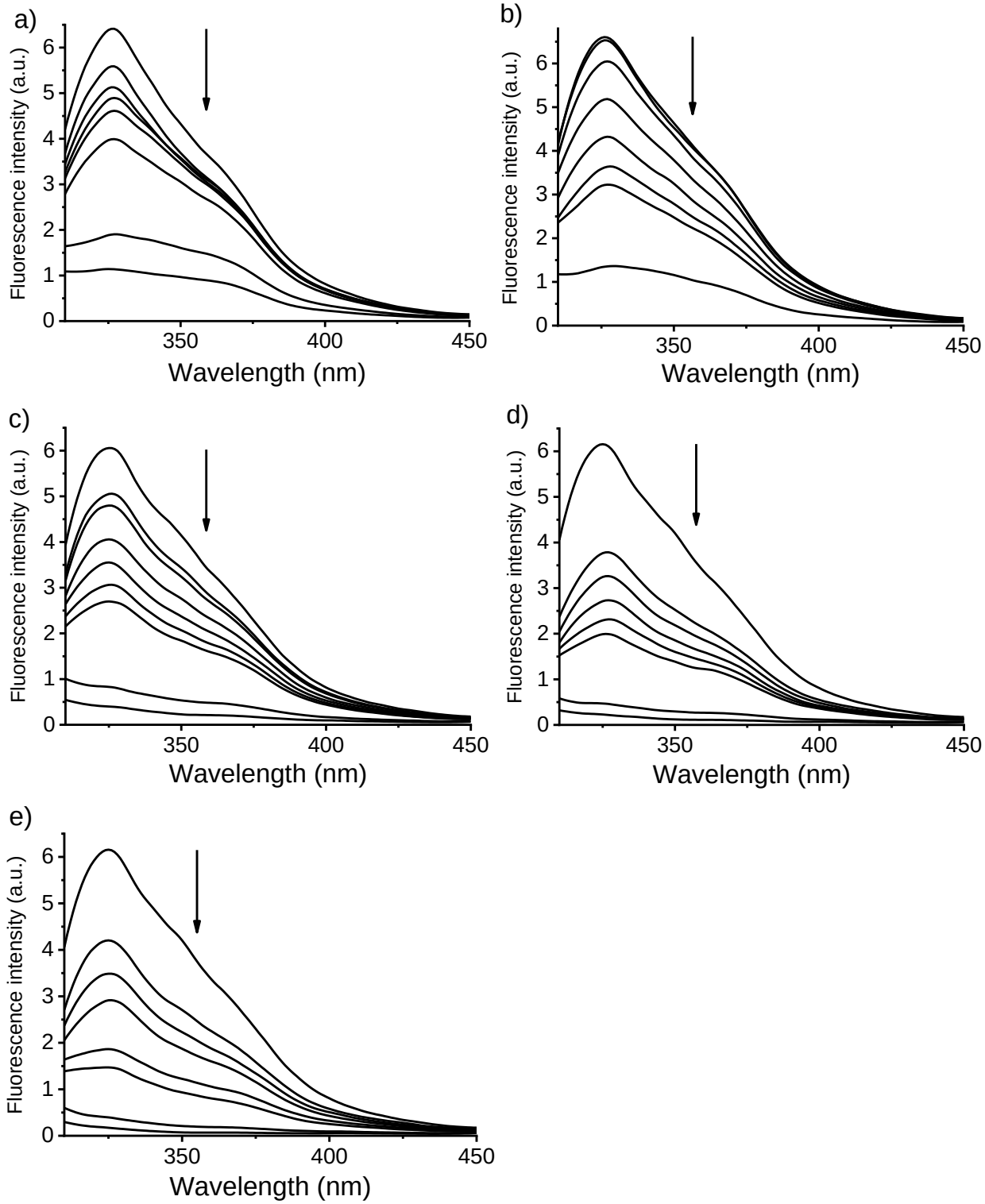

Figure S19. Albumin fluorescence quenching spectra of the Cu(II) complexes **1a** (a), **2a** (b), **4a** (c), **5a** (d), **6a** (e).

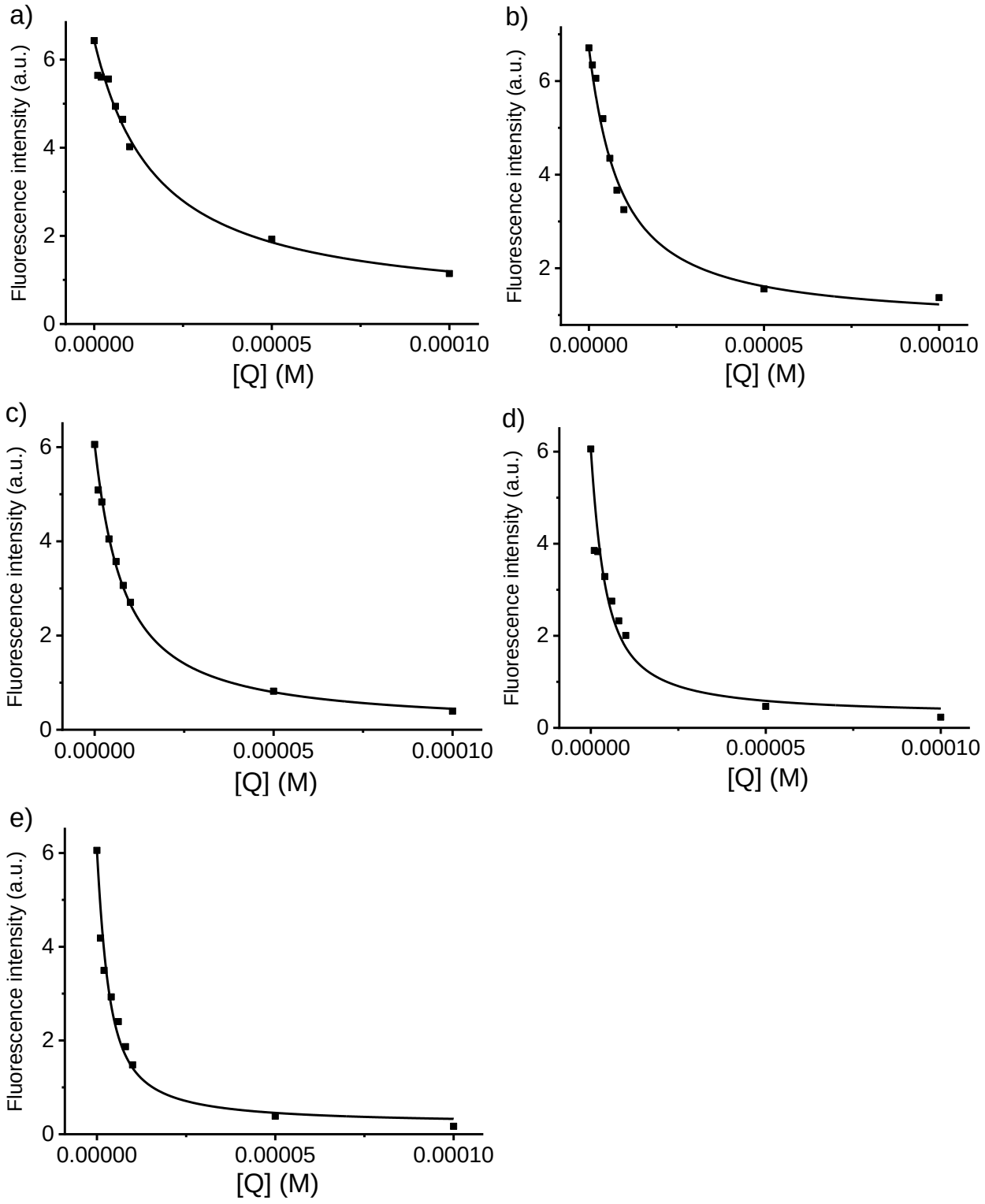

Figure S20. Non-linear regression analysis for albumin fluorescence quenching of the Cu(II) complexes **1a** (a, $R^2 = 0.98268$), **2a** (b, $R^2 = 0.98433$), **4a** (c, $R^2 = 0.99446$), **5a** (d, $R^2 = 0.91987$), **6a** (e, $R^2 = 0.96730$).

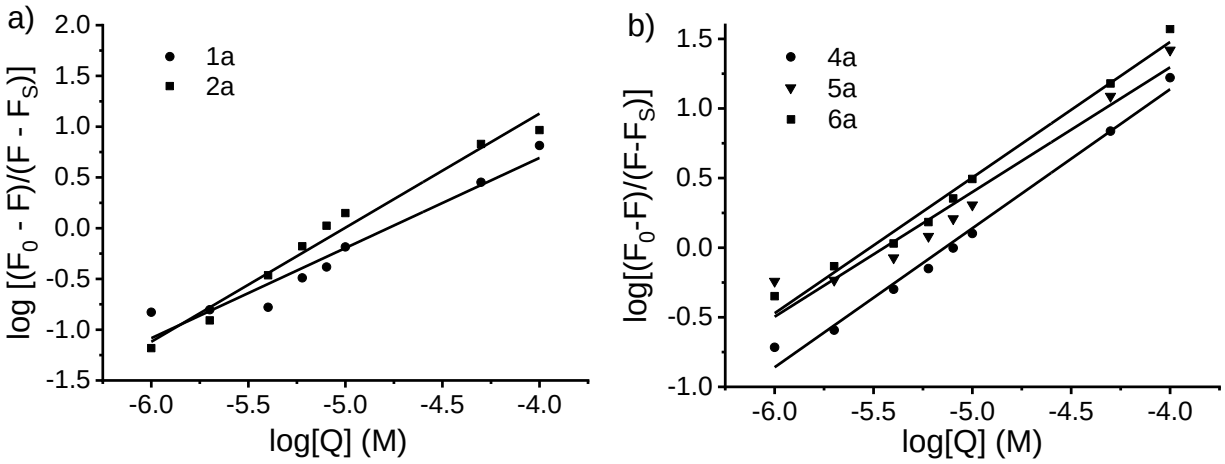

Figure S21. The Hill plots for albumin fluorescence quenching of the Cu(II) complexes **1a** (R^2 = 0.93154), **2a** (R^2 = 0.97388) (a); **4a** (R^2 = 0.98584), **5a** (R^2 = 0.94190), **6a** (R^2 = 0.98187) (b).

Hemoglobin binding studies

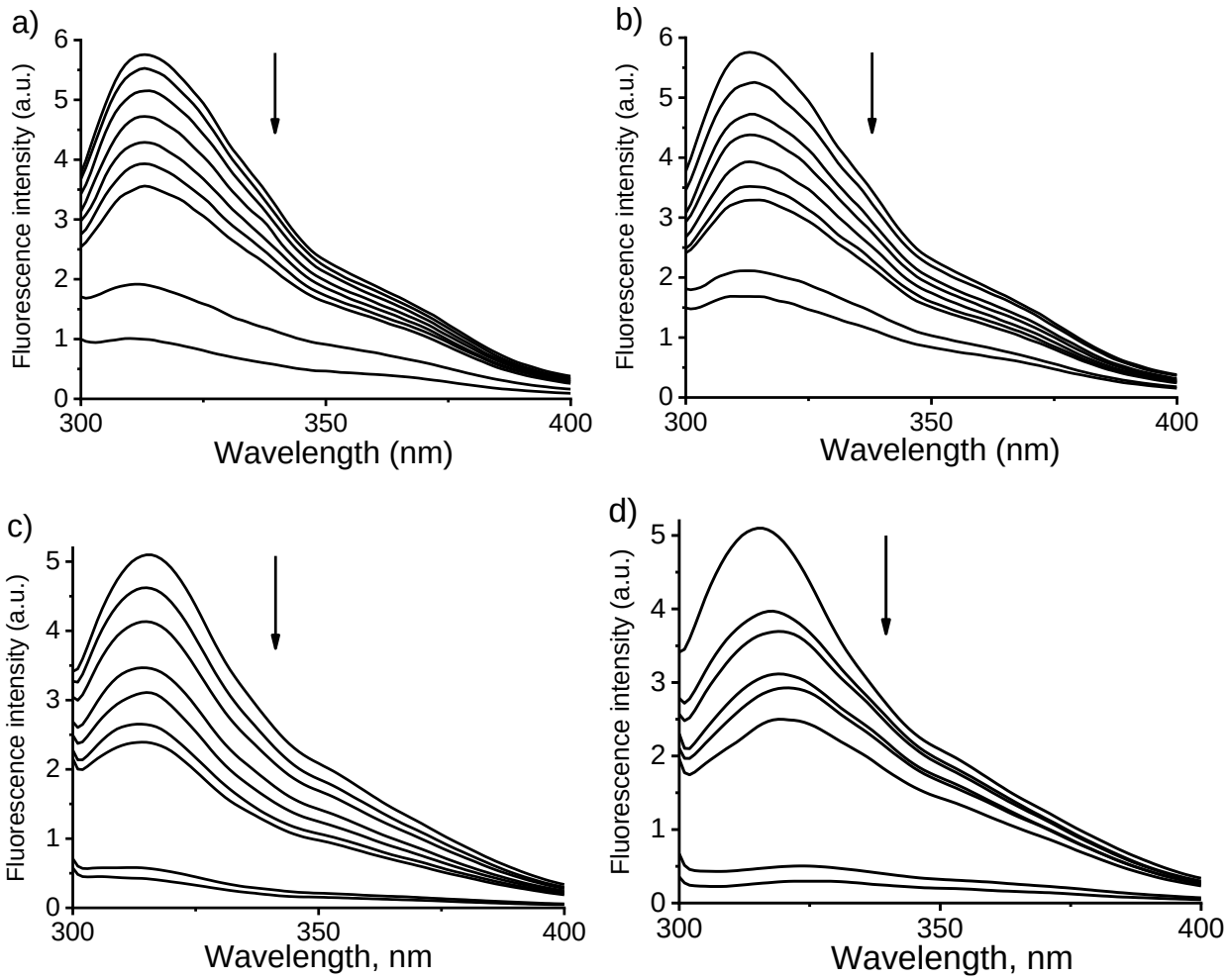

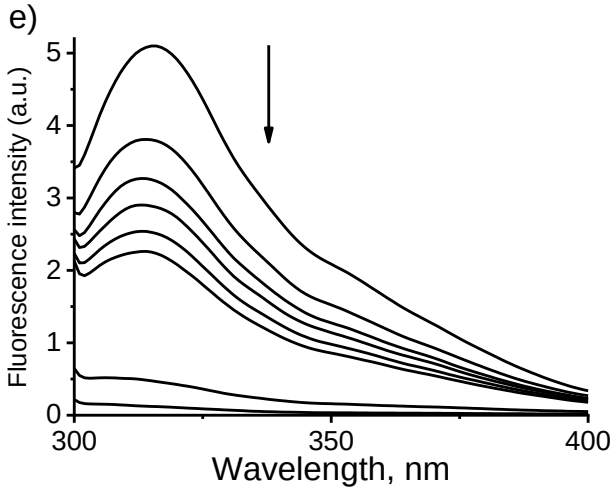

Figure S22. Hemoglobin fluorescence quenching spectra of the Cu(II) complexes **1a** (a), **2a** (b), **4a** (c), **5a** (d), **6a** (e).

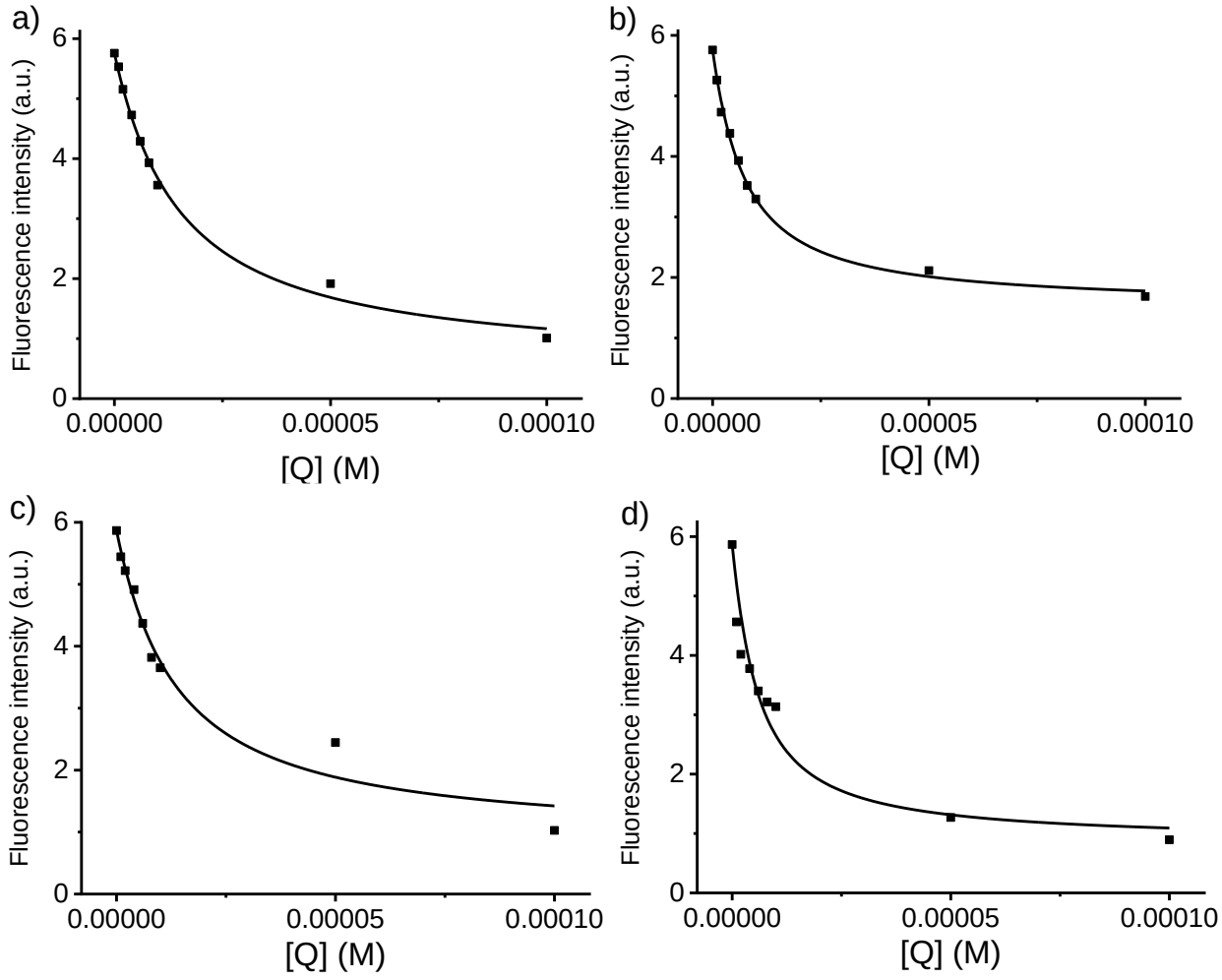

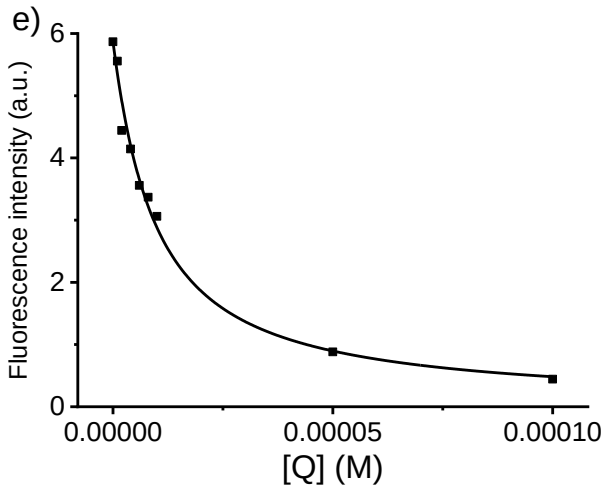

Figure S23. Non-linear regression analysis for hemoglobin fluorescence quenching of the Cu(II) complexes **1a** (a, R^2 = 0.99450), **2a** (b, R^2 = 0.99535), **4a** (c, R^2 = 0.96710), **5a** (d, R^2 = R^2 = 0.92648), **6a** (e, R^2 = 0.98623).

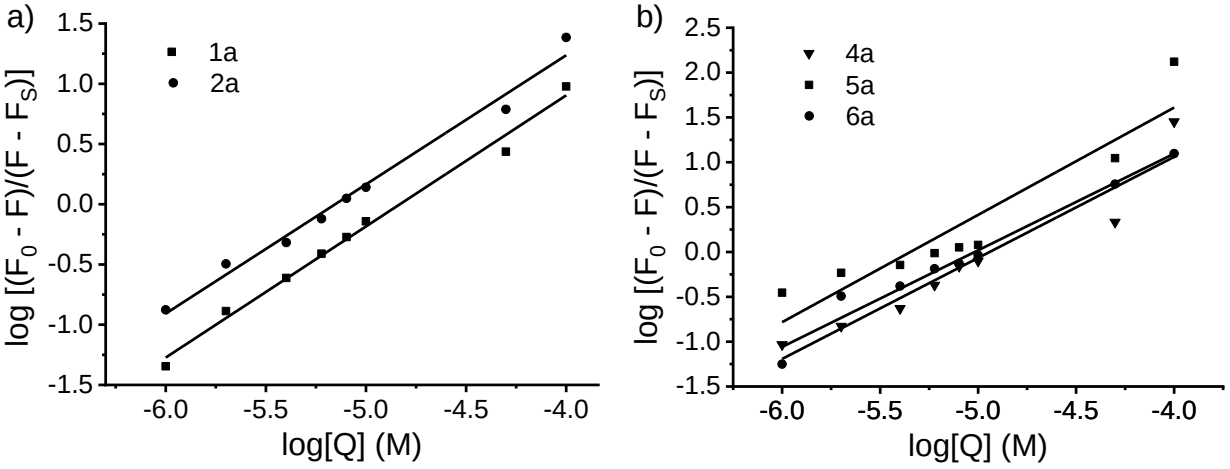

Figure S24. The Hill plots for hemoglobin fluorescence quenching of the Cu(II) complexes **1a** (R^2 = 0.98872), **2a** (R^2 = 0.98304) (a); **4a** (R^2 = 0.90603), **5a** (R^2 = 0.85135), **6a** (R^2 = 0.96794) (b).

DFT calculations

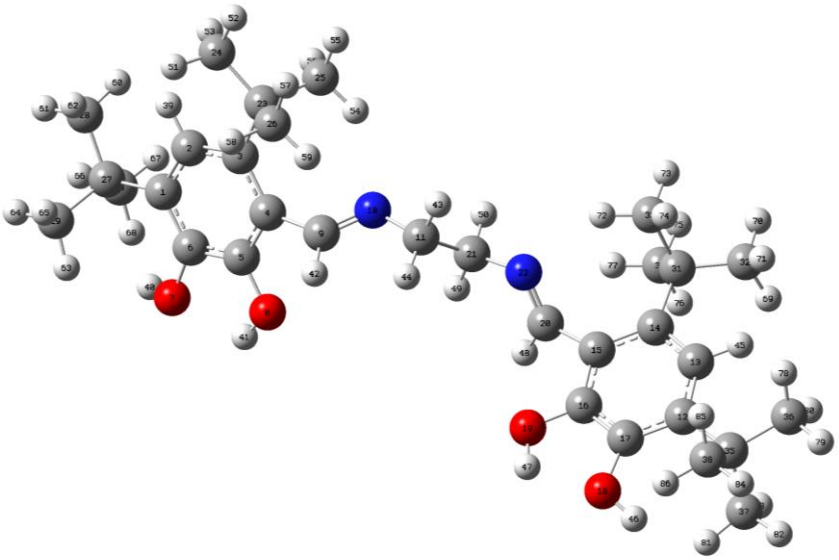

Figure S25. DFT-optimized structure of the ligand **1**.

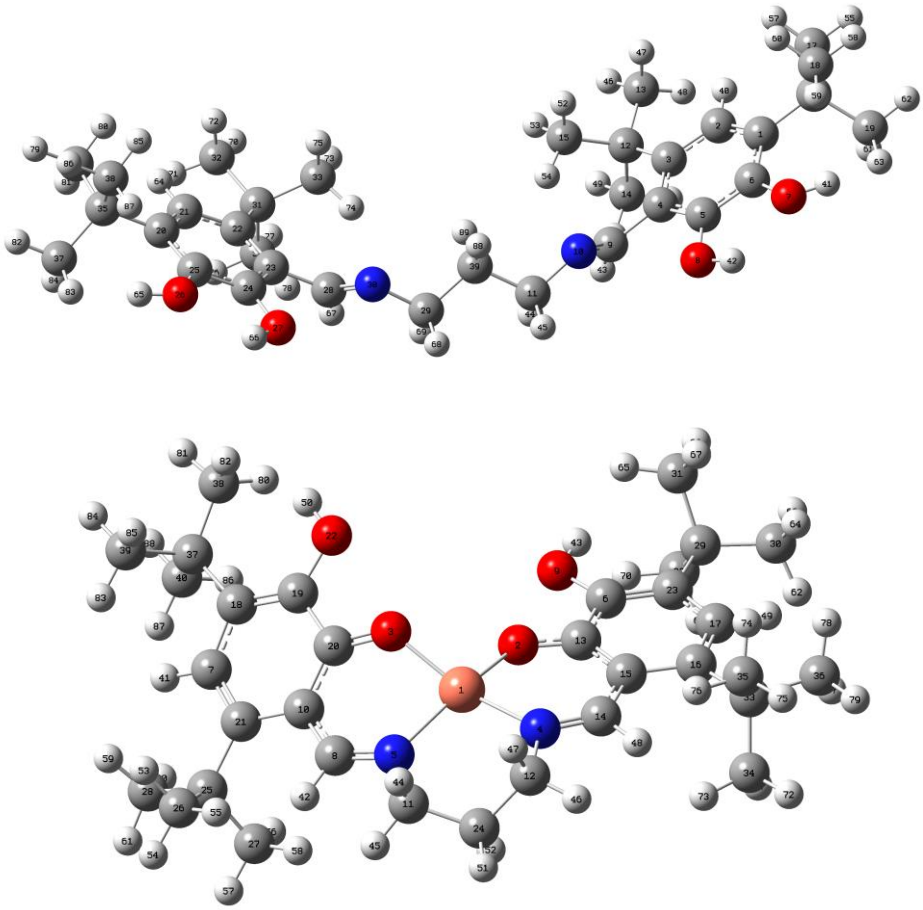

Figure S26. DFT-optimized structures of the ligand **2** and the complex **2a**.

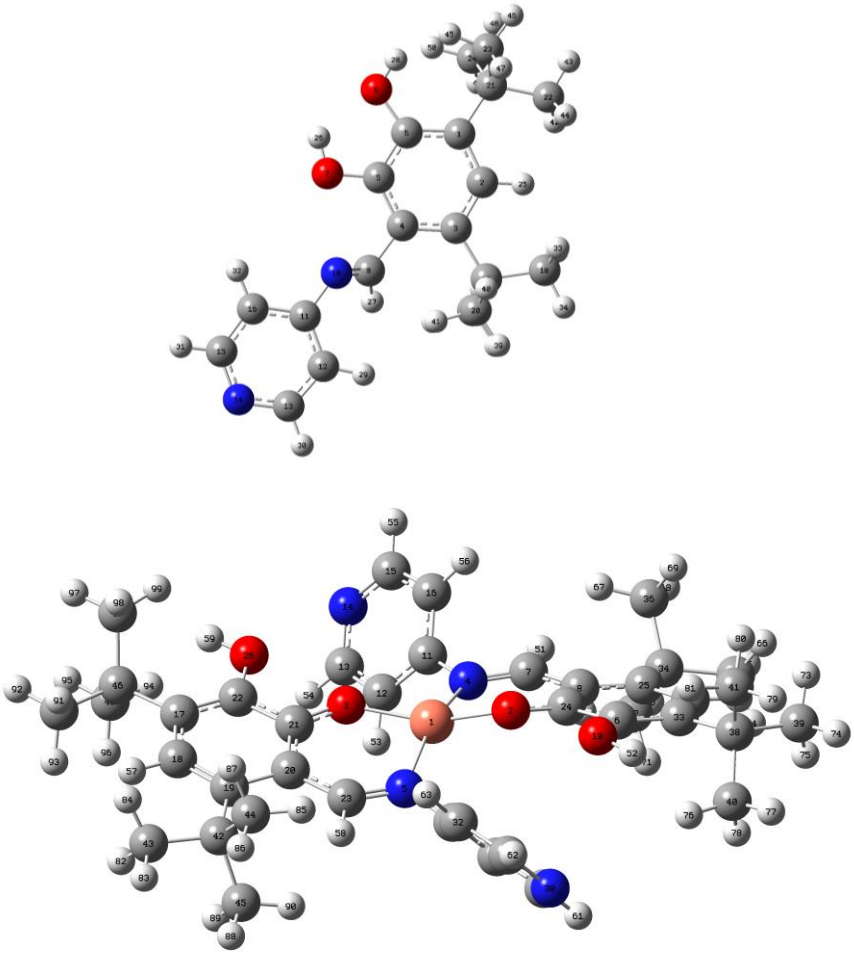

Figure S27. DFT-optimized structures of the ligand **3** and the complex **3a**.

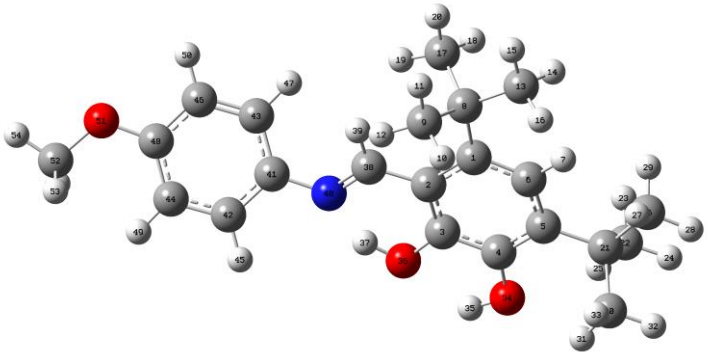

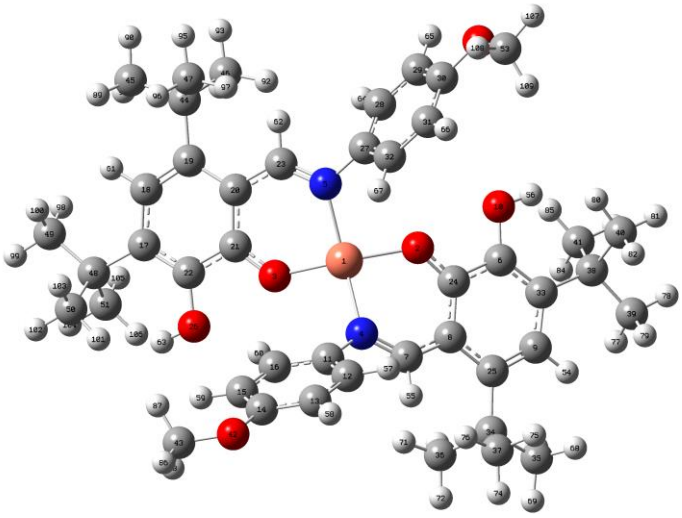

Figure S28. DFT-optimized structures of the ligand **4** and the complex **4a**.

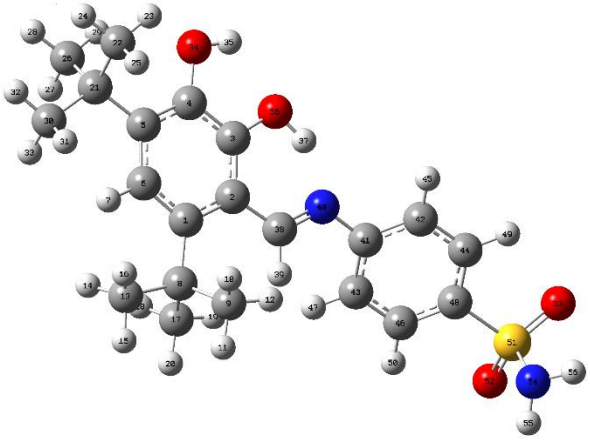

Figure S29. DFT-optimized structure of the ligand **5**.

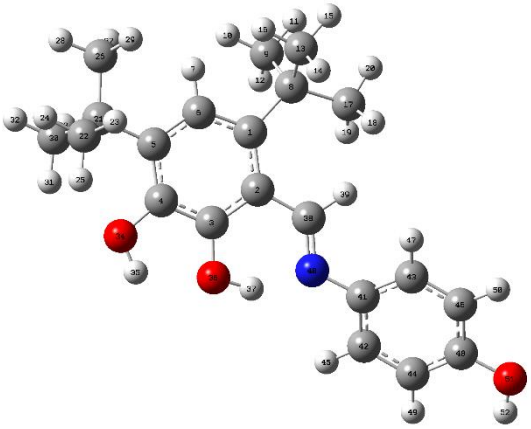

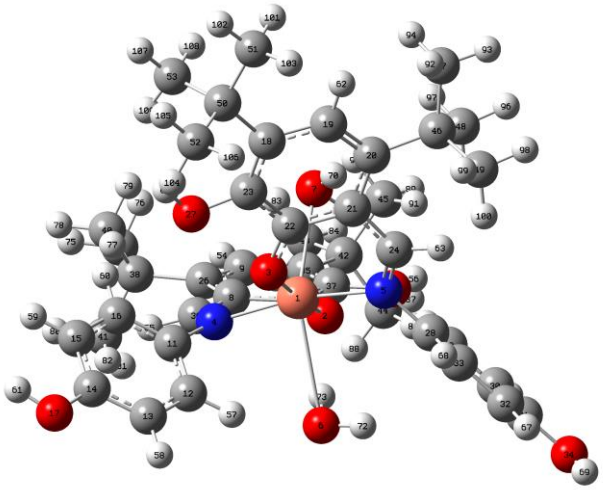

Figure S30. DFT-optimized structure of the ligand **6** and the complex **6a**.

Table S3. Prominent IR absorption bands (ν, cm^{-1}) of the ligands and their Cu(II) complexes.

Compound		ν(N–H)	ν(O–H)	ν(C=N)	ν(C_{arom}–N)	ν(C–O)	ν(Cu–O)	ν(Cu–N)
1	Exp.	–	3398s	1613s	1243m 1221m	1196m 1132m	–	–
	Calcd.	–	3716	1659	1246 1212	1186 1124	–	–
1a	Exp.	–	3314s	1618s	1289m 1234m	1192m 1103m	623m	463w
	Calcd.	–	3355	1599	1306 1220	1207 1082	601	488
2	Exp.	–	3498s 3368s	1615s	1243m 1219m	1198m 1114m	–	–
	Calcd.	–	3715 3626	1656	1269 1229	1189 1123	–	–
2a	Exp.	–	3502s 3308s	1595s	1305m 1233m	1164m 1110m	619m	470w
	Calcd.	–	3663 3640	1584	1311 1235	1145 1064	591	474
3	Exp.	–	3100s	1583s	1230m 1205m	1169m 1073m	–	–
	Calcd.	–	3621	1638	1223 1218	1190 1016	–	–
3a	Exp.	–	3375s	1578s	1248m 1228m	1165m 1086m	601m	488w
	Calcd.	–	3639 3631	1576	1254 1215	1140 1054	610	468
4	Exp.	–	3365s 3343s	1590s	1220m	1189m 1111m	–	–
	Calcd.	–	3595	1592	1228	1188 1149	–	–
4a	Exp.	–	3342s	1587s	1262m 1241m	1166m 1090m	618m	488w
	Calcd.	–	3637	1591	1253 1210	1138 1052	593	438
5	Exp.	3415s 3375s	3279s	1585s	1250m 1223m	1161m 1097m	–	–
	Calcd.	3483 3380	3600	1583	1260 1224	1184 1147	–	–
5a	Exp.	3401s 3351s	3270s	1579s	1263m 1227m	1158m 1090m	618m	488w
	Calcd.	3423 3320	3635	1552	1266 1210	1135 1053	588	490
6	Exp.	–	3339s 3255s 3171s	1619s 1606s	1242m 1222m	1161m 1108m 1039m	–	–

	Calcd.	–	3693 3592 2773	1593	1237 1224	1181 1148 1051	–	–
6a	Exp.	–	3392s	1585s	1259m 1225m	1165m 1090m	622m	482w
	Calcd.	–	3639	1575	1253 1211	1135 1049	588	473

Table S4. DFT-calculated parameters for the Cu(II) complexes.

Computed Parameter	Compound					
	1a	**2a**	**3a**	**4a**	**5a**	**6a**
Dipole moment (D)	7.578	2.359	1.044	1.196	6.901	3.837
MO energy (kcal/mol)						
HOMO	-115.24	-107.33	-116.08	-107.59	-119.16	-111.06
LUMO	-38.21	-26.36	-38.20	-29.73	-40.27	-31.13
ΔE	77.03	80.97	77.88	77.86	78.89	79.93
Bond length (Å)						
Cu(1)–O(2)	1.912	1.917	1.903	1.913	1.906	1.957
Cu(1)–O(3)	1.912	1.921	1.906	1.917	1.905	1.926
Cu(1)–N(4)	1.967	1.997	2.033	2.025	2.032	2.035
Cu(1)–N(5)	1.967	2.013	2.013	2.017	2.029	2.084
Cu(1)–O(6)	-	-	-	-	-	2.904
Cu(1)–O(7)	-	-	-	-	-	2.600
Bond angles (°)						
N(4)–Cu(1)–O(2)	-	89.7	88.7	88.9	89.2	86.4
N(4)–Cu(1)–O(3)	90.2	-	96.3	97.5	96.5	92.7
O(3)–Cu(1)–N(5)	-	87.7	89.7	89.7	89.3	86.2
N(5)–Cu(1)–O(2)	90.2	-	93.2	94.0	96.5	95.9
O(2)–Cu(1)–O(3)	95.1	90.9	-	-	-	-
N(4)–Cu(1)–N(5)	84.9	98.6	-	-	-	-
N(4)–Cu(1)–O(6)	-	-	-	-	-	82.3
N(4)–Cu(1)–O(7)	-	-	-	-	-	105.3
N(5)–Cu(1)–O(6)	-	-	-	-	-	88.2
N(5)–Cu(1)–O(7)	-	-	-	-	-	86.1

O(2)–Cu(1)–O(6)	-	-	-	-	-	68.0
O(2)–Cu(1)–O(7)	-	-	-	-	-	80.3
O(3)–Cu(1)–O(6)	-	-	-	-	-	118.0
O(3)–Cu(1)–O(7)	-	-	-	-	-	94.0

Molecular docking studies

Table S5. Binding energies and amino acid surroundings of the Cu(II) complexes upon protein binding.

Compound	E_{bind}, kcal/mol	AA surrounding within 4 Å
PDB code: 6ick		
4a	-8.4	LYS(239), PHE(281), ASN(187), THR(181), VAL(237), ASP(184), TYR(240), LEU(182), PHE(174), HIS(278), PHE(171), PHE(223), GLY(180)
PDB code: 2f00		
5a	-8.1	ARG(10), LEU(39), ARG(117), VAL(13), ILE(22), PRO(104), SER(80), ARG(17), VAL(19), GLU(15), GLU(42), ARG(119), GLU(114), PHE(118), TYR(44), PRO(14), LEU(115)
PDB code: 4jk4		
5a (1)	-7.4	LYS(131), GLU(16), LYS(51), PHE(36), LYS(132), ASP(129), GLY(135), ASP(37), TRP(134), VAL(40), GLU(17), LYS(20), ASN(44), LYS(41), GLU(48), LEU(24)
5a (2)	-7.1	ASP(124), LYS(136), TYR(137), PRO(35), GLU(140), PHE(36), ASP(118), ALA(128), GLU(125), ASP(37), TYR(160), ARG(143), LEU(115), TYR(139), THR(121)
5a (3)	-7.1	LYS(294), ARG(194), THR(190), LYS(187), ASP(450), GLU(293), VAL(292), GLU(186), GLU(291), SER(191), GLU(443), ARG(435), TYR(156)
4a (1)	-7.8	GLU(478), PHE(205), GLY(206), ARG(208), LYS(350), LYS(204), ALA(209), LEU(480), LEU(346), GLU(353), SER(479), VAL(481), THR(477), GLU(357)
4a (2)	-7.1	VAL(228), PHE(227), ARG(208), THR(231), ALA(321), GLU(320), VAL(234), ALA(324), ASP(323), THR(235), LYS(211), VAL(215)
4a (3)	-7.0	LEU(115), LYS(136), ARG(185), ILE(181), PRO(113), LYS(116), GLU(140), TYR(137), LEU(122), PHE(133), GLU(125), TYR(160), PRO(117), ARG(143), ASP(118)
PDB code: 6ihx		

5a	-6.8	TYR(140), PRO(95), VAL(93), THR(134), SER(138), ASP(94), THR(137), LYS(99), ARG(92), SER(133)
6a	-6.6	SER(81), LEU(83), ALA(79), LYS(68), GLU(82), LYS(61), LEU(80), THR(67), HEM(201), GLU(71), ALA(64), ALA(65)

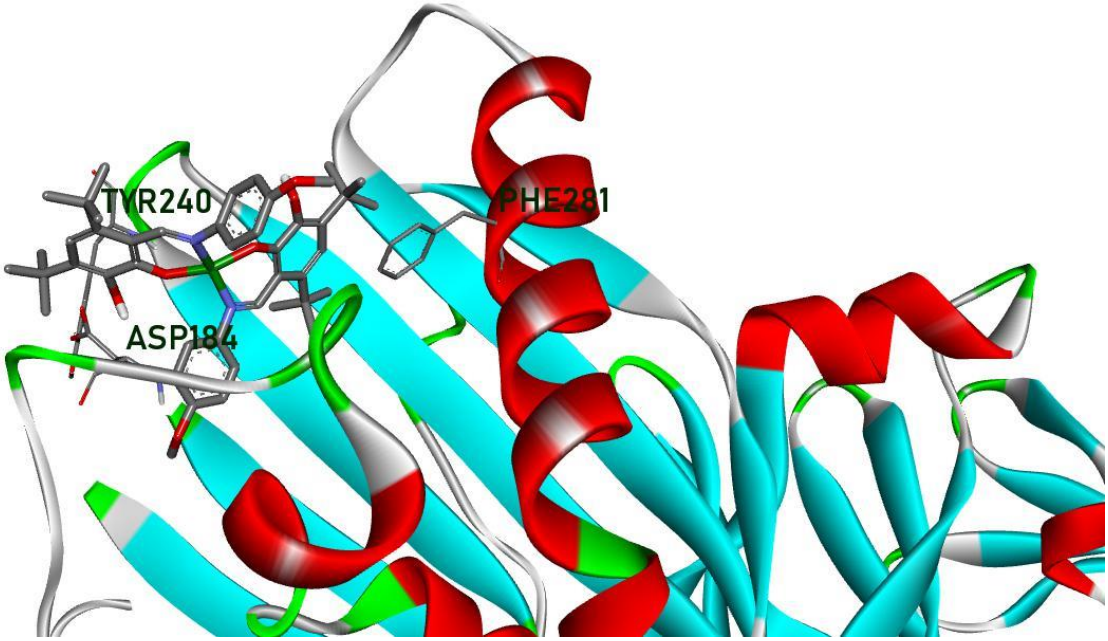

Figure S31. Interaction of the compound **4a** with metal binding protein (PDB code: 6ick).

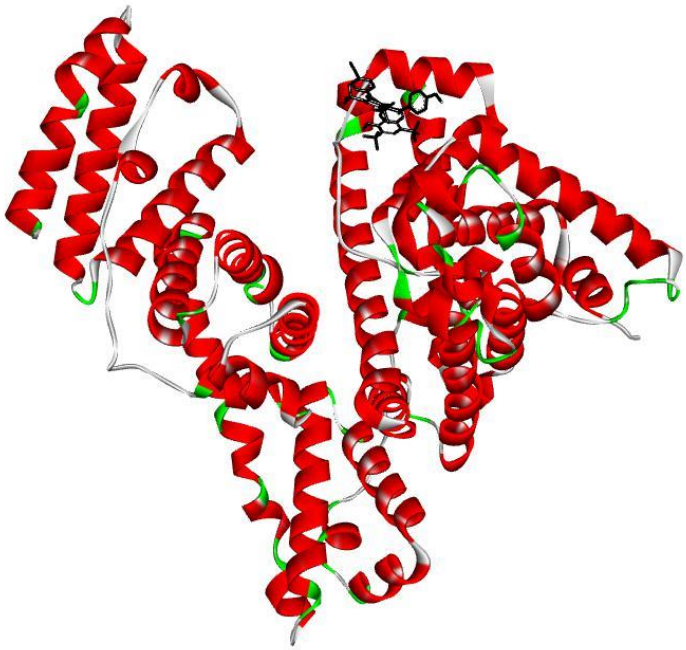

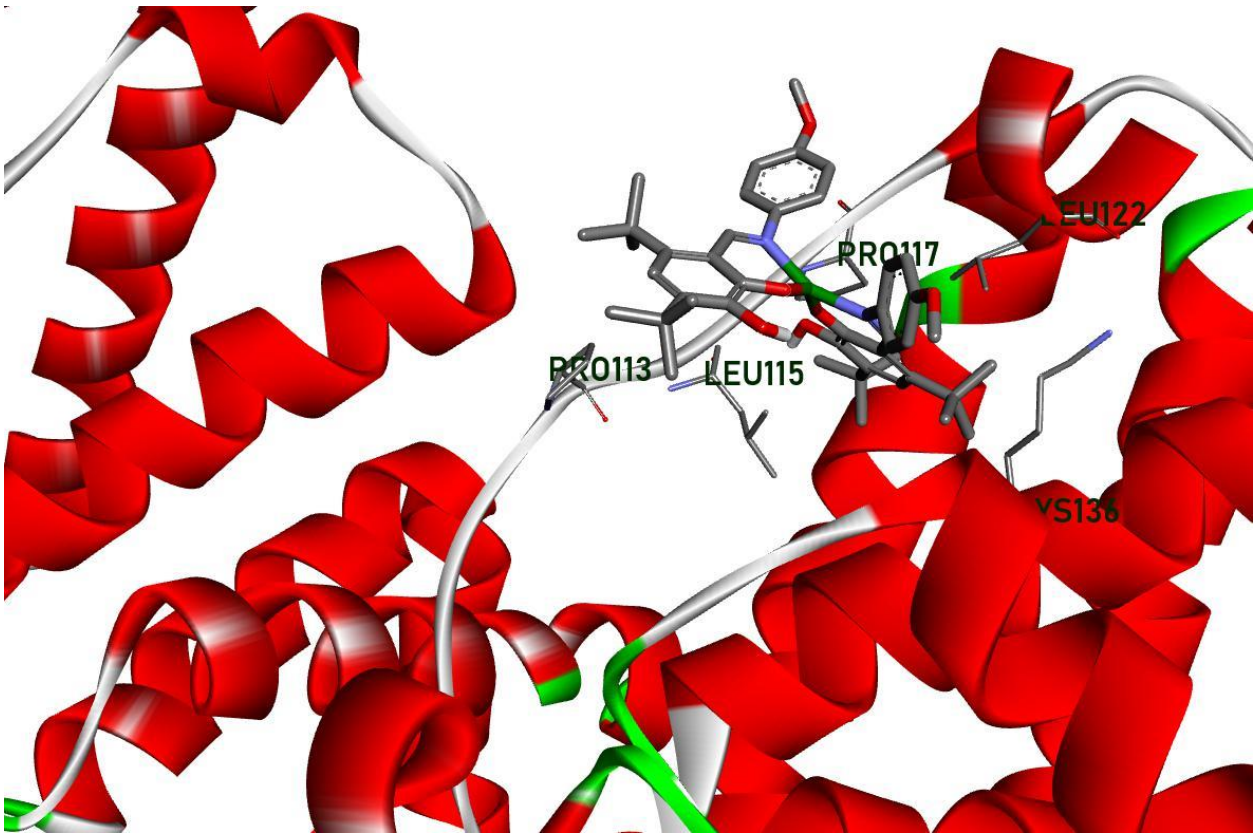

Figure S32. Interaction of the compound **4a** (3) with bovine serum albumin (PDB code: 4jk4).

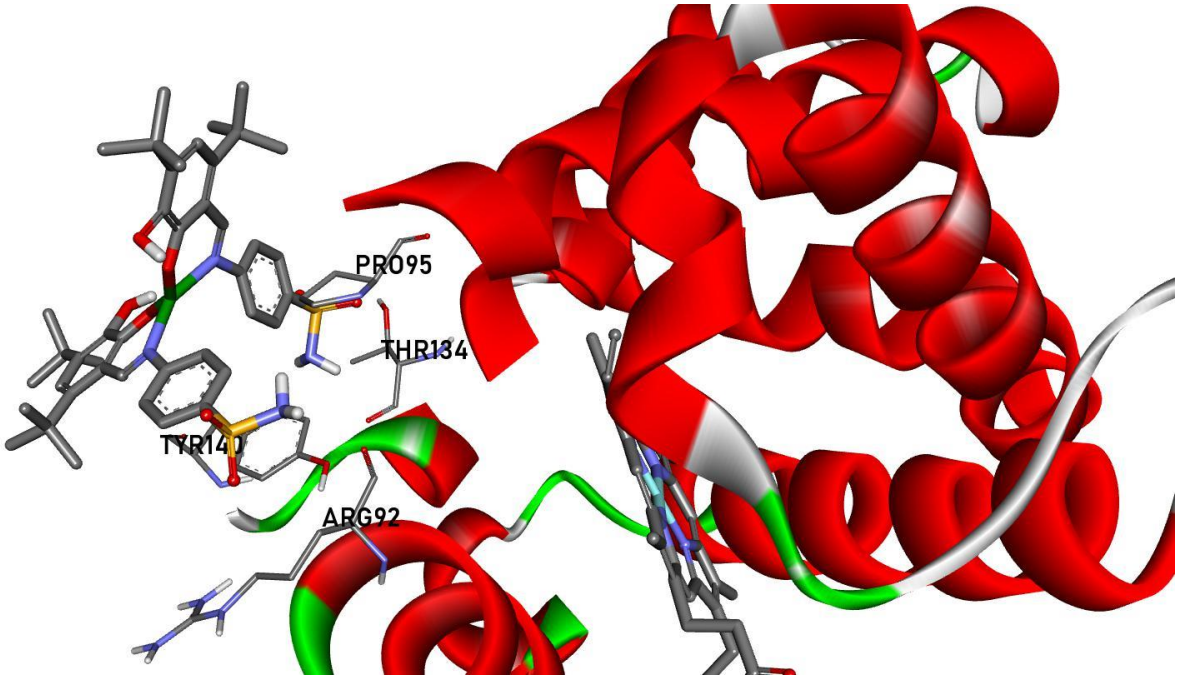

Figure S33. Interaction of the compound **5a** (3) with bovine hemoglobin (PDB code: 6ihx).

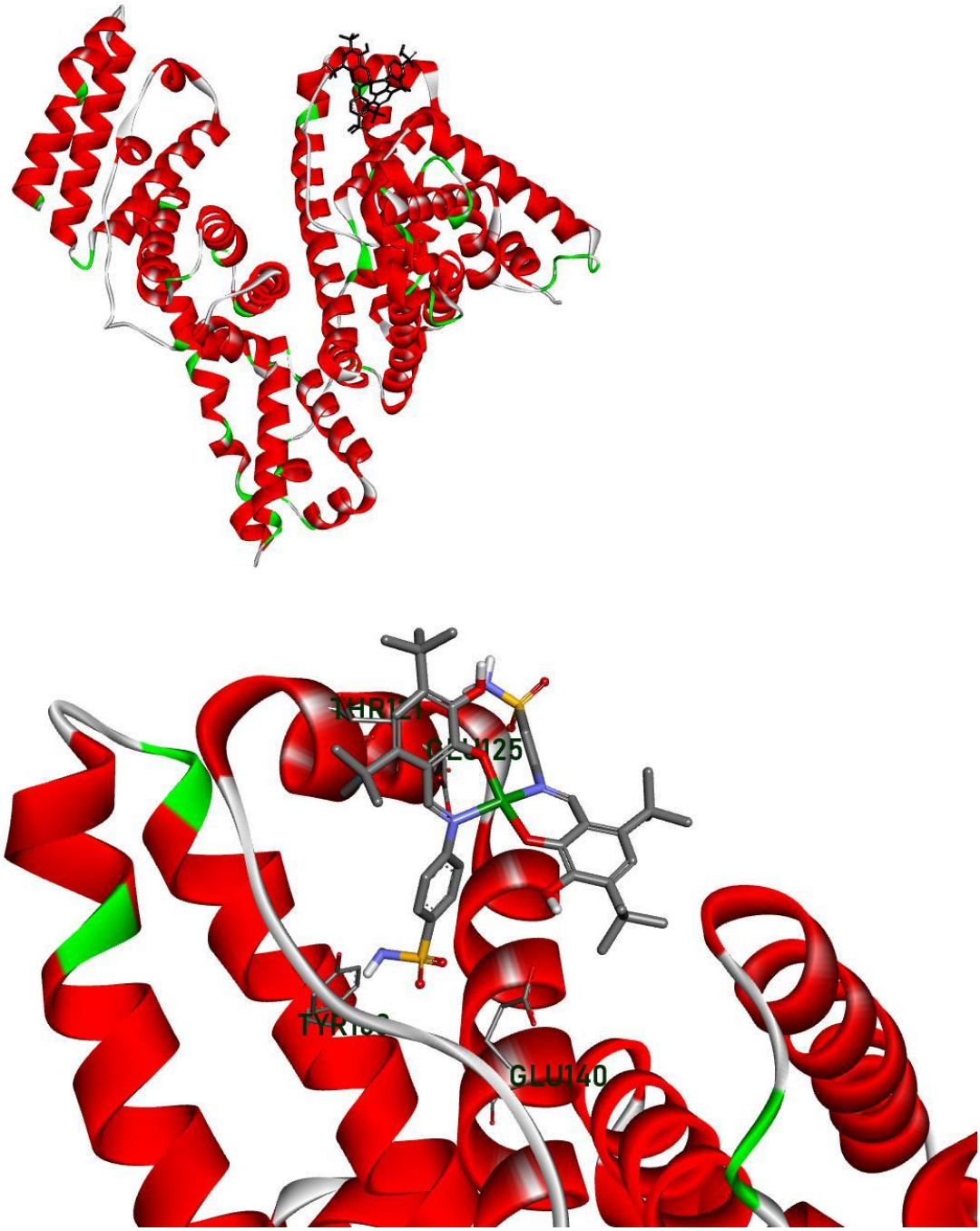

Figure S34. Interaction of the compound **5a** (2) with bovine serum albumin (PDB code: 4jk4).

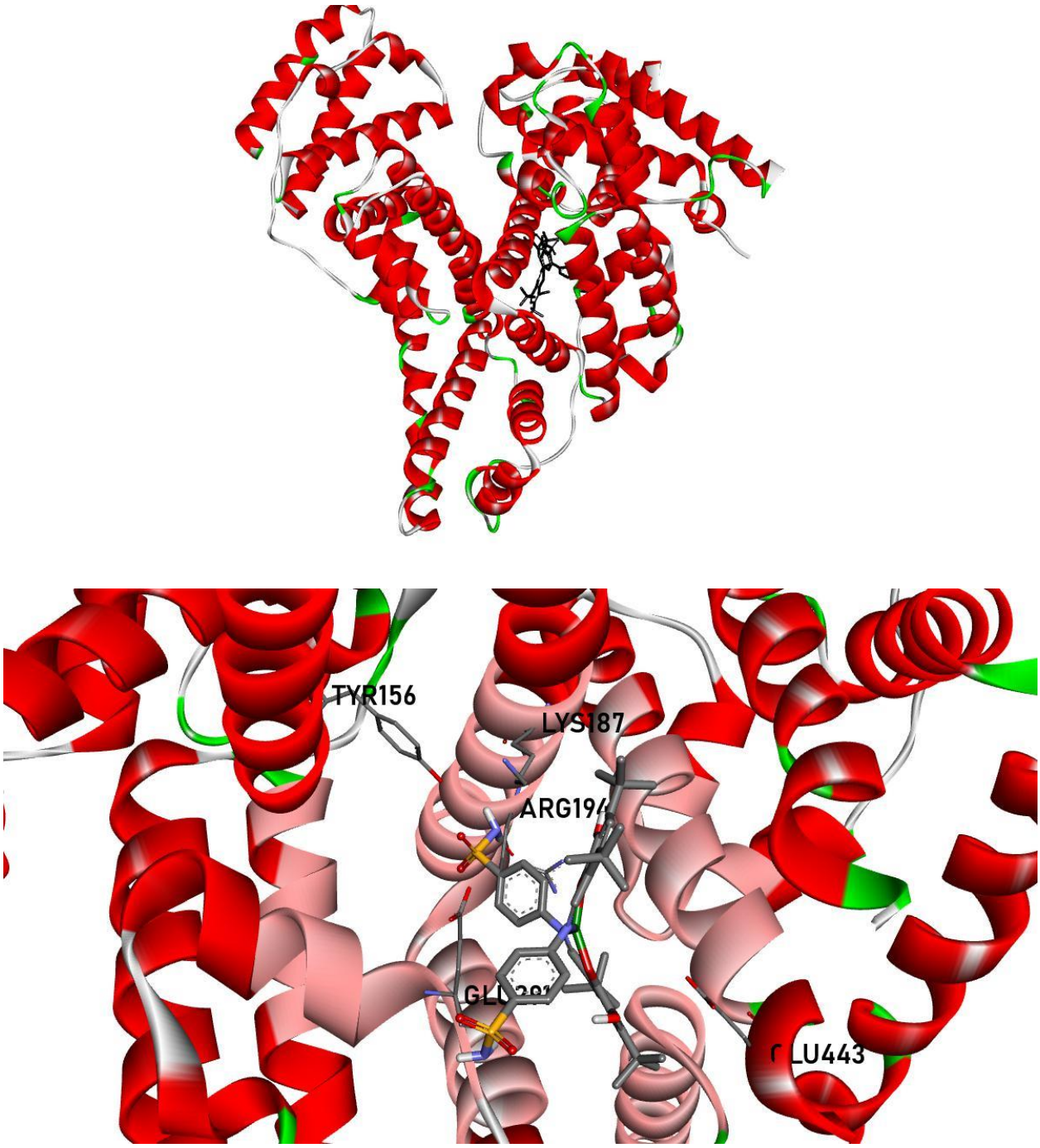

Figure S35. Interaction of the compound **5a** (3) with bovine serum albumin (PDB code: 4jk4).

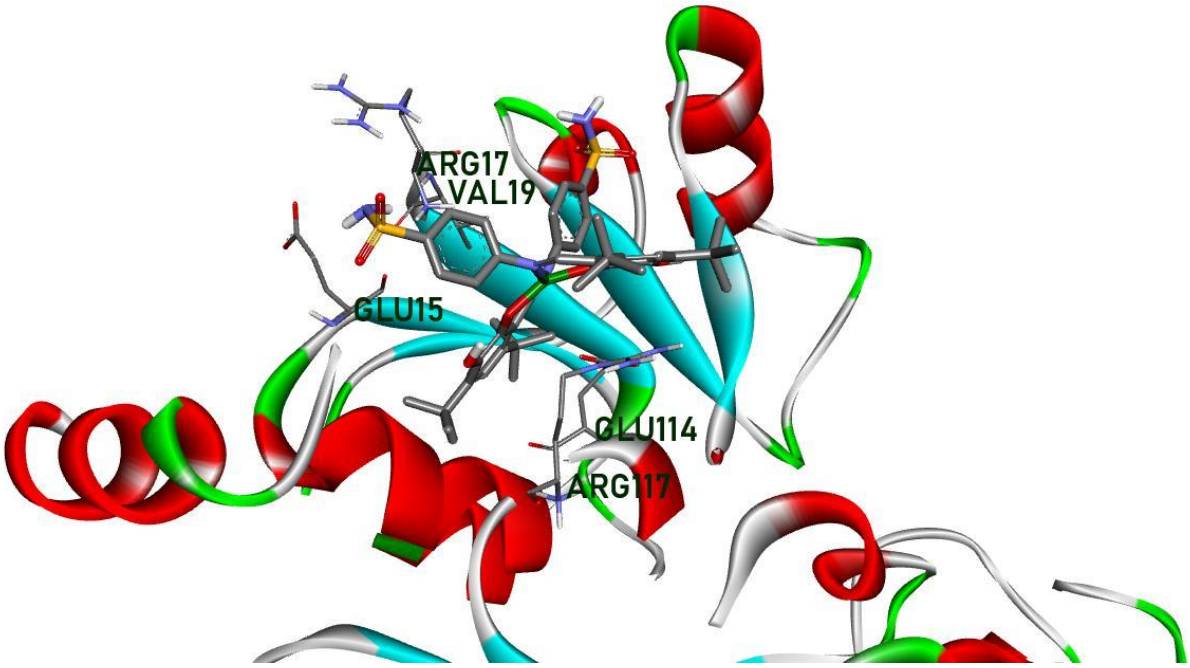

Figure S36. Interaction of the compound **5a** with the MurC protein (PDB code: 2f00).

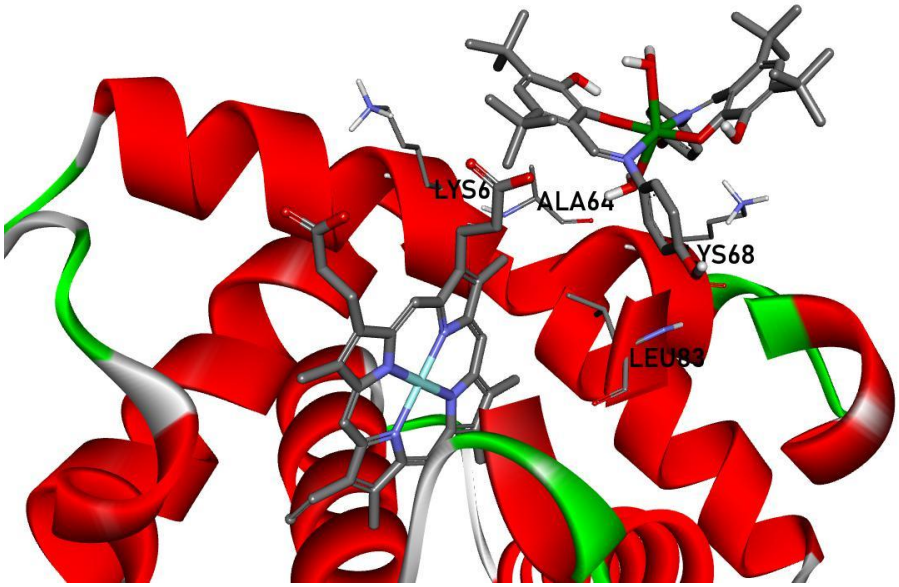

Figure S37. Interaction of the compound **6a** with bovine hemoglobin (PDB code: 6ihx).

Table S6. Experimental and calculated dissociation constants of the Cu(II) complexes for the compound-protein complexes with albumin and hemoglobin.

Compound	Albumin		Hemoglobin	
	K_d experimental, M^{-1}	K_d calculated, M^{-1} 298K	K_d experimental, M^{-1}	K_d calculated, M^{-1} 298K
1a	$(1.61 \pm 0.25)\cdot 10^{-5}$	$1.90 \cdot 10^{-6}$	$(1.39 \pm 0.12)\cdot 10^{-5}$	$2.84 \cdot 10^{-5}$
2a	$(7.76 \pm 1.06)\cdot 10^{-6}$	$7.34 \cdot 10^{-6}$	$(6.38 \pm 0.45)\cdot 10^{-6}$	$2.02 \cdot 10^{-5}$

4a	$(6.81 \pm 0.52)\cdot10^{-6}$	$6.20 \cdot10^{-6}$	$(7.68 \pm 0.33)\cdot10^{-6}$	$1.71 \cdot10^{-5}$
5a	$(2.96 \pm 0.89)\cdot10^{-6}$	$3.74 \cdot10^{-6}$	$(8.82 \pm 1.11)\cdot10^{-6}$	$1.03 \cdot10^{-5}$
6a	$(2.21 \pm 0.47)\cdot10^{-6}$	$3.74 \cdot10^{-6}$	$(6.67 \pm 0.79)\cdot10^{-6}$	$1.44 \cdot10^{-5}$

References

1. M.Y. Gvozdev, N.V. Loginova, G.A. Ksendzova, N.P. Osipovich, T.V. Koval'chuk-Rabchinskaya, Y.V. Faletrov, A.M. Khodosovskaya, A.N. Evtushenkov, *Medicinal Chemistry*, 2022.

2. D. Beckett, *Methods in Enzymology*, 2011, **488**.